# Implications of the seismic source dynamics for the characteristics of a possible tsunami in a model problem of the seismic gap in the Central Kurile region

L. I. Lobkovsky, and B. V. Baranov

P. P. Shirshov Institute of Oceanology, Russian Academy of Sciences, Moscow, Russia

R. Kh. Mazova, and L. Yu. Kataeva

Nizhny Novgorod State Technical University, Nizhniy Novgorod, Russia

Received 15 October 2006; accepted 28 October 2006; published 28 November 2006.

[1] Various scenarios of earthquakes and the associated tsunami wave generation are numerically simulated. It is shown that, depending on the chosen dynamic source parameters in the central seismic gap zone of the Kurile-Kamchatka arc, the characteristics of tsunami waves in the water area of the Sea of Okhotsk and Kurile-Kamchatka zone can differ dramatically, from insignificant inundation of Sakhalin and Kamchatka coasts to a catastrophic run-up of waves up to 8 m in height. Detailed numerical constraints on the tsunami wave run-up are obtained for a number of points of the Sakhalin coastline, the form of the first waves climbing the coast is determined, and the run-up velocity characteristics are computed. *INDEX TERMS:* 3025 Marine Geology and Geophysics: Marine seismics; 3060 Marine Geology and Geophysics: Subduction zone processes; 3285 Mathematical Geophysics: Wave propagation; 4255 Oceanography: General: Numerical modeling; 4564 Oceanography: Physical: Tsunamis and storm surges; *KEYWORDS:* tsunami generation, submarine landslide, sedimentary mass, elasto-plastic model, shallow water equations.

**Citation:** Lobkovsky, L. I., B. V. Baranov, R. Kh. Mazova, and L. Yu. Kataeva (2006), Implications of the seismic source dynamics for the characteristics of a possible tsunami in a model problem of the seismic gap in the Central Kurile region, *Russ. J. Earth. Sci., 8,* ES5002, doi:10.2205/2006ES000209.

## Introduction

[2] This work is devoted to a comprehensive study of the possible generation of a strong tsunami in the seismic gap region of the Kurile Islands subduction zone on the basis of field data gathered during the Kurile-2005 marine scientific expedition in the zone of seismic gap of the Kurile-Kamchatka arc (Figure 1). A top priority problem is the situational modeling of possible sources of tsunamigenic earthquakes and the analysis of possible scenarios of the generation of tsunami waves leading to catastrophic consequences [*Mazova et al.,* 1983]. Thus, one of the tasks of tsunami zonation is the situational modeling of a seismic source, the determination of the related hydrodynamic parameters of tsunami sources, calculations of the tsunami wave motion in an ocean with the real bathymetry, and estimation of characteristic parameters of the tsunami wave run-up at a given coastline.

[3] The formation of tsunami is known to depend on the mode and dynamics of seafloor displacements in the earthquake source zone (more specifically on the initial displacements of the seafloor). The calculations of the tsunami wave generation are generally based on seismic data used for the determination of the source rupture orientation and the tsunami energy [*Mazova and Ramirez,* 1999]. The static problem of calculating the ocean surface motion from the distribution of seafloor movements is then solved. The resulting displacements of the water surface are regarded as initial conditions and the propagation of a wave in a given water area is calculated, with the real bathymetry taken into account. The presently existing numerical models and software complexes (e.g. see [*Goto et al.,* 1997]) allow one to calculate rather accurately the propagation of the tsunami wave toward the coast. After the Indian Ocean tsunami of 26 December, 2004, the accuracy of such calculations can be assessed by comparing 3-D model distribution


ISSN: 1681–1208 (online)

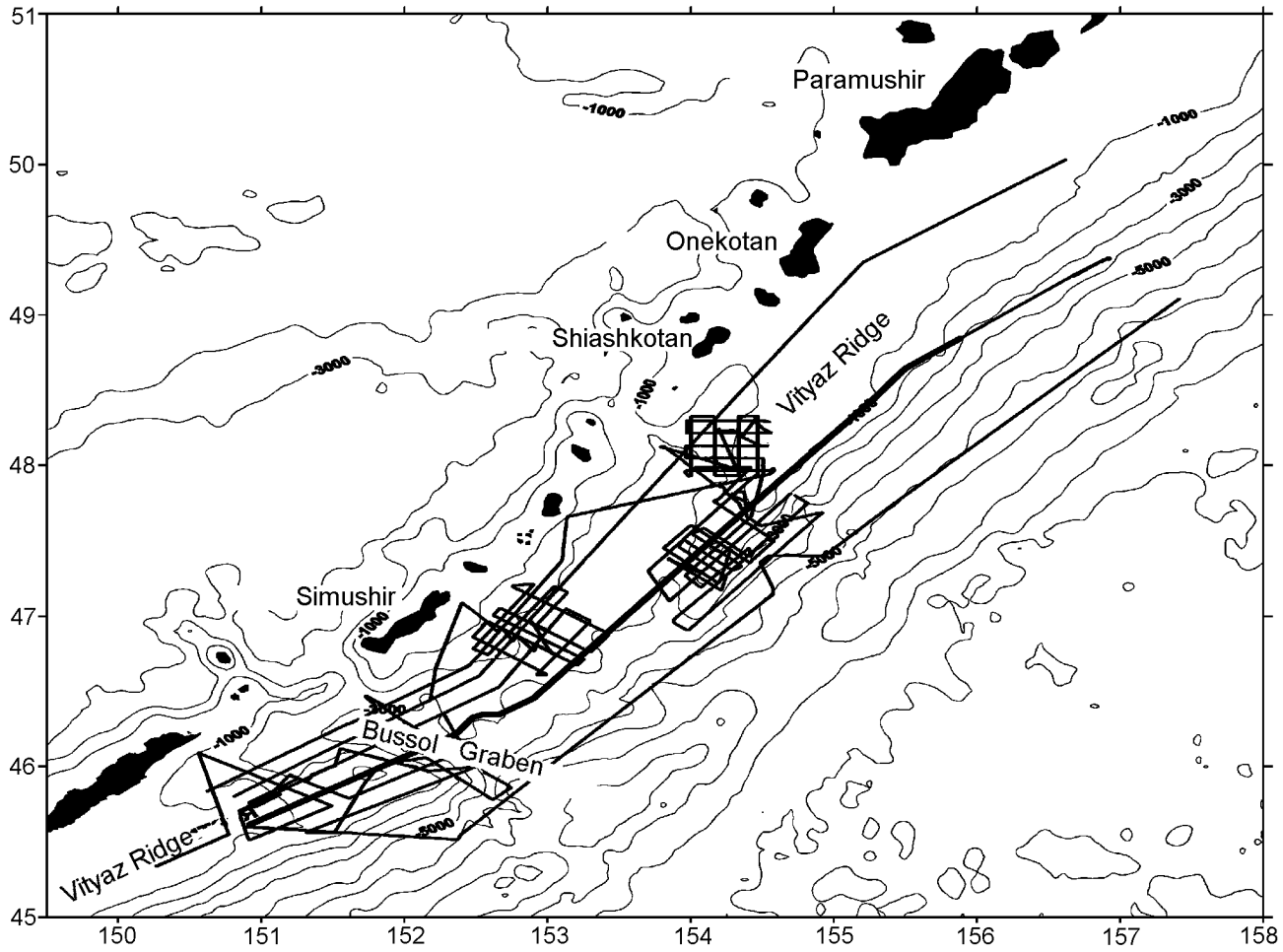


**Figure 1.** Location of geophysical profiles (gray lines) in the seismic gap zone (the Kurile-2005 expedition); the black line is the profile shown in Figure 2; the isobath interval is 1000 m.

in the Indian Ocean with satellite data on the water displacements induced by tsunami propagation [*Laverov et al.,* 2006a]. However, these calculations involve the problem of adequacy of the source model in use. Specific features of the tsunami generation such as its initial velocity, parameters, and coastal characteristics (particularly, in the near-field zone) are directly dependent on the choice of the model for the determination of an earthquake source [*Levin,* 1978].

[4] At present, the mechanism of strong earthquakes in subduction zones has been developed [*Lobkovsky,* 1988; *Lobkovsky and Baranov,* 1984; *Lobkovsky et al.,* 2004]. It is known that narrow seismic belt of the Earth are related to the contact conditions at boundaries of large lithospheric plates. The interaction of plates in the underthrusting zone is responsible for the seismic process in island arcs and at active continental margins. The strongest earthquakes occur in subduction zones and in the vicinity of the contact plane dipping at a low angle between the island arc uplift base and the top of the underthrust plate. Numerous geomorphological, geological, and geophysical data indicate that the island arc uplift consists of large segments formed by transverse faults extending down to the top of the underthrust plate. For example, traces of these faults are well seen in Figure 2, presenting a part of the seismic profile that illustrates the structure of the central Kurile arc slope in the area explored by the Kurile-2005 expedition (the 37th cruise of the R/V Akademik Lavrentyev) [*Laverov et al.,* 2006b]. The presence of transverse faults required the introduction of new, smaller elements of interaction, namely, blocks ("keyboard-blocks") at the frontal edge of the overhanging plate. It was found out that this minimal complication of the traditional subduction scheme is sufficient to account for the main features of the seismic process in subduction zones [*Lobkovsky et al.,* 2004]. The characteristic size of the keyboard-blocks is about 100 km. This block fragmentation of frontal parts of island arc and continental margins is a structural factor controlling the source size of a strong earthquake [*Fedotov,* 1968]. Such sources are mostly related to deformed keyboard-blocks "shooting" at the time moment of stress release. However, sometimes the source of a very strong earthquake is comparable in length to a few neighboring blocks simultaneously releasing the accumulated elastic energy. It can be supposed that eight or ten keyboard-blocks of the Sunda island arc "jumped" simultaneously in December 2004, and the great

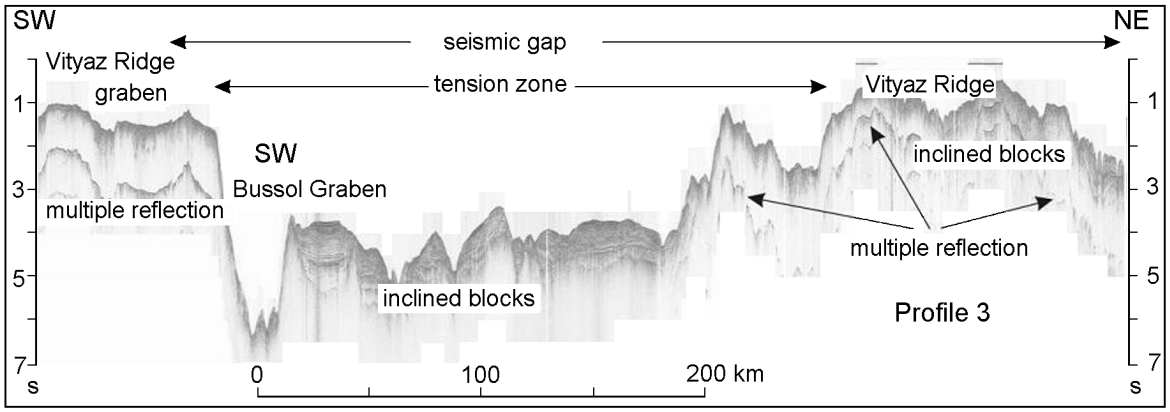


**Figure 2.** Seismic profile 3 illustrating the block structure of the frontal part of the central Kurile-Kamchatka island arc (position of the profile is shown in Figure 1).

amount of the related released energy resulted in the formation of a huge earthquake source, giving rise to a giant tsunami.

[5] The deep-sea trench located on the oceanward side of the Southern Kuriles makes the Kurile Islands region a potentially hazardous seismic zone, particularly because submarine earthquakes in a subduction zone are generally tsunamigenic. Tsunamis generated by such earthquakes are hazardous for coastal areas of the Sea of Okhotsk (including Sakhalin Island) where both industrial and residential structures are located. Several tsunami attacks of the Sakhalin coast caused by earthquakes in the Kurile Islands region have been fixed historically [*Burymskaya and Ivashchenko,* 1985; *Burymskaya and Vyalykh,* 1985; *Solovyev,* 1978]. Although the tsunami intensity is largely controlled by the strength of a submarine earthquake, the wave heights on the Sakhalin coast rarely reached the record values known in the history of tsunami on the Pacific coast [*Ikonnikova,* 1963; *Solovyev et al.,* 1977; *Vasilyev and Shchetnikov,* 1985; *L. I. Lobkovsky et al.,* 2006]. For example, at the Sakhalin coast, the wave due to the Urup earthquake of 13 October, 1963 was no more than half a meter high [*Shchetnikov,* 1990]. This is primarily due to the fact that the tsunami wave propagation toward Sakhalin is hindered by high submarine ridges (such as the Vityaz Ridge) separating the Sea of Okhotsk water area from tsunami sources in the deep-sea trench zone; as a result, the deep-sea Bussol and Kruzenshtern straits are the only natural tsunami waveguides.

[6] The distribution of earthquake sources along the Kurile Island arc is nonuniform. Whereas the sources are distributed uniformly in the southern and northern parts of the Kurile arc, no submarine earthquakes have been observed for a long time in the central Kurile region, i.e. this is a seismic gap zone [*Fedotov and Chernyshev,* 2002; *Laverov et al.,* 2006a]. Such a situation seems to be fairly dangerous because, the oceanic plate being thrust under the continental plate at an average velocity of 6–8 cm $yr^{-1}$, significant elastic stresses could have accumulated in the subduction zone. In the southern and northern parts of the Kurile arc, the underthrusting-induced release of elastic energy over the past period was gradual due to small-block structure of the deep-sea trench there, while the elastic energy release process in the central Kurile zone can lead to a strong submarine earthquake that in turn is capable of causing the tsunami of a significant destructive potential. The probability of such an event is supported by the fact that, as is known, the source of the Indian Ocean tsunami of 26 December, 2004 was also located in the area of the deep-sea trench near coasts of Indonesia, and the subduction zone in the area where the oceanic plate moves under the Sunda and Indo-Australian plates was seismically quiescent for more than 200 years, which has resulted in the catastrophic aftermath of the elastic energy release process. In the Russian territory, an event of this type is possible in the central part of the Kurile-Kamchatka subduction zone extending in the NE direction for more than 200 km from Simushir Island.

## Model Used for Calculating the Movements of Submarine Keyboard-Blocks Generating Tsunami

[7] The position of the possible source of a tsunamigenic earthquake is determined from the data gathered during the Kurile-2005 expedition (Figures 1 and 2) [*Laverov et al.,* 2006b]. The depth of the submarine ridge slope varies from 1.5 km to 4.5 km. As is clearly seen, the strongly dissected submarine Vityaz Ridge reminds blocks in the keyboard model of a tsunamigenic earthquake [*Lobkovsky,* 1988; *Lobkovsky and Baranov,* 1984; *Lobkovsky et al.,* 2004]. These blocks are about 25–50 km long. However, there are known examples illustrating that seismogenic blocks group with time within the same zone of subduction [*Lobkovsky,* 1988]; i.e. an earthquake source can encompass several blocks, and in this case the earthquake magnitude and source rupture length increase. A similar scenario of the seismic process development appears to have realized as the December 2004 catastrophe on Sumatra Island (Indonesia). The source of the earthquake was more than 1000 km long and involved several blocks.

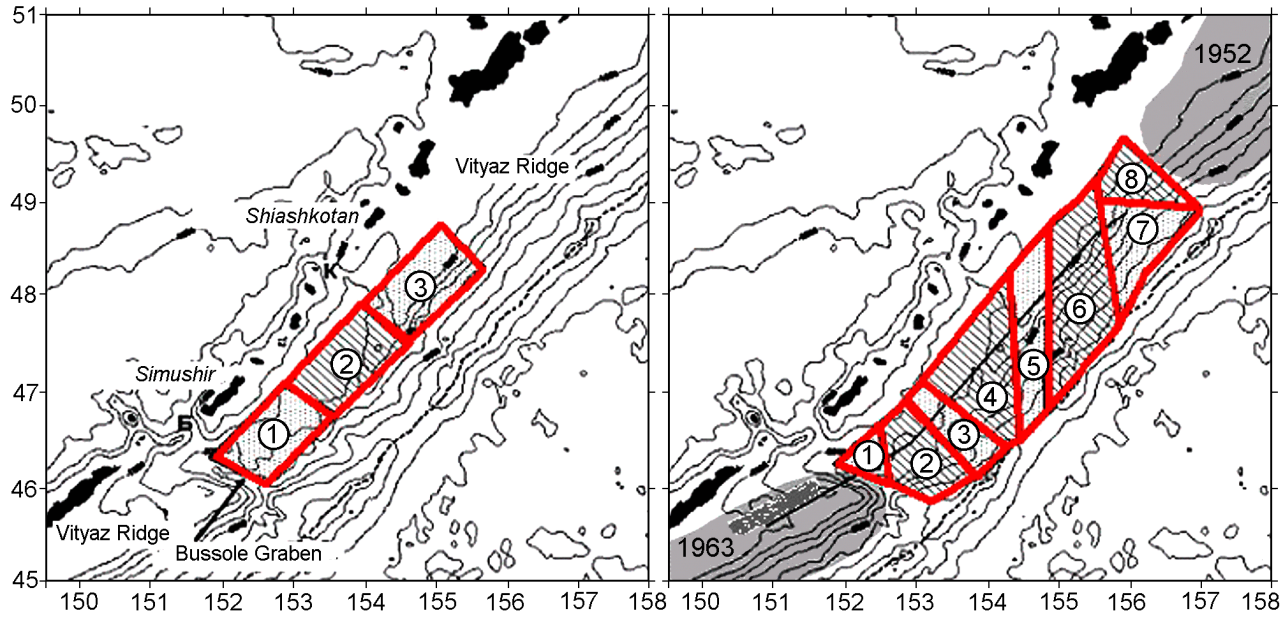


**Figure 3.** Location of model seismic sources consisting of three blocks (left panel) and eight blocks (right panel). In the second case, the block parameters were constrained by data obtained in the Kurile-2005 expedition. The broken line is the trench axis.

[8] To model the possible earthquake, we chose two types of a hypothetical earthquake source having lengths of about 330 km and 465 km and located between the Bussol Strait and Shiashkotan Island with widths of about 70 km and 130 km, respectively, so that the source is similar to a curvilinear figure with cross section (3) along its median line (Figure 3). The average distances of the model sources to the Kurile-Kamchatka islands amount to about 35 km and 25 km, respectively. In both cases, we considered sources consisting of various numbers of keyboard-blocks (from 3 to 8) capable of moving in the vertical direction. The average vertical velocity of the blocks varied from 0.15 m $s^{-1}$ to 1 m $s^{-1}$, depending on the characteristic time of the motion in the source. The amplitudes of downward and upward movements of the blocks varied from 5 m to 14 m. Horizontal block movements were not considered. The propagation of the waves generated on the water surface was calculated up to 10-m isobath.

## Model Used for Simulation of Tsunami Waves Generated by Displacements of Submarine Keyboard-Blocks

[9] The wave generation and propagation were described by the nonlinear system of equations of shallow water [*Pelinovsky,* 1982; *Pelinovsky and Mazova,* 1992; *Voltsinger et al.,* 1989]

$$\begin{cases} \mathbf{U}_t + \mathbf{U}\cdot\operatorname{grad}\mathbf{U} + g\cdot\operatorname{grad}\eta = \mathbf{F} \\ \eta_t + \operatorname{div}\Big(\big(H+\eta-B\big)\mathbf{U}\Big) = B_t \end{cases} \tag{1}$$

$$\mathbf{F} = \begin{pmatrix} fv - g\dfrac{u\sqrt{u^2+v^2}}{Ch^2\big(H+\eta-B\big)} \\ -fu - g\dfrac{v\sqrt{u^2+v^2}}{Ch^2\big(H+\eta-B\big)} \end{pmatrix},\ \mathbf{U} = \begin{pmatrix} u \\ v \end{pmatrix},$$

where $\eta$ is the water surface displacement, $H$ is the basin depth, and $u$ and $v$ are the components of the horizontal wave velocity, $f = 2\Omega\cos\theta$ is the Coriolis parameter, $\Omega$ is the Earth's angular velocity, $\theta$ is the geographical latitude, $g$ is the gravity acceleration, $Ch = \dfrac{(H+\eta-B)^{0.4}}{sh}$ is the Chesie coefficient, $sh$ is the asperity coefficient, and the function $B(x,y,t)$ describes the motion of the basin floor.

### Numerical Scheme

[10] Of the variety of difference schemes approximating equations (1), we chose the scheme proposed in [*Marchuk et al.,* 1983] because of its high algorithmic versatility. The scheme is based on a divided difference and, in conjunction with the central difference approximation of spatial derivatives, simplifies the numerical implementation of boundary conditions:

$$\eta_{ij}^{n+1} =$$

$$\eta_{ij}^{n} + \Delta t_j\Big(\frac{1}{2\cdot\Delta x_p}\big(u_{ij+1}^{n}\cdot\big(H_{ij+2}^{n}+H_{ij+1}^{n}\big) - u_{ij}^{n}\cdot\big(H_{ij+1}^{n}+H_{ij}^{n}\big)\big)$$

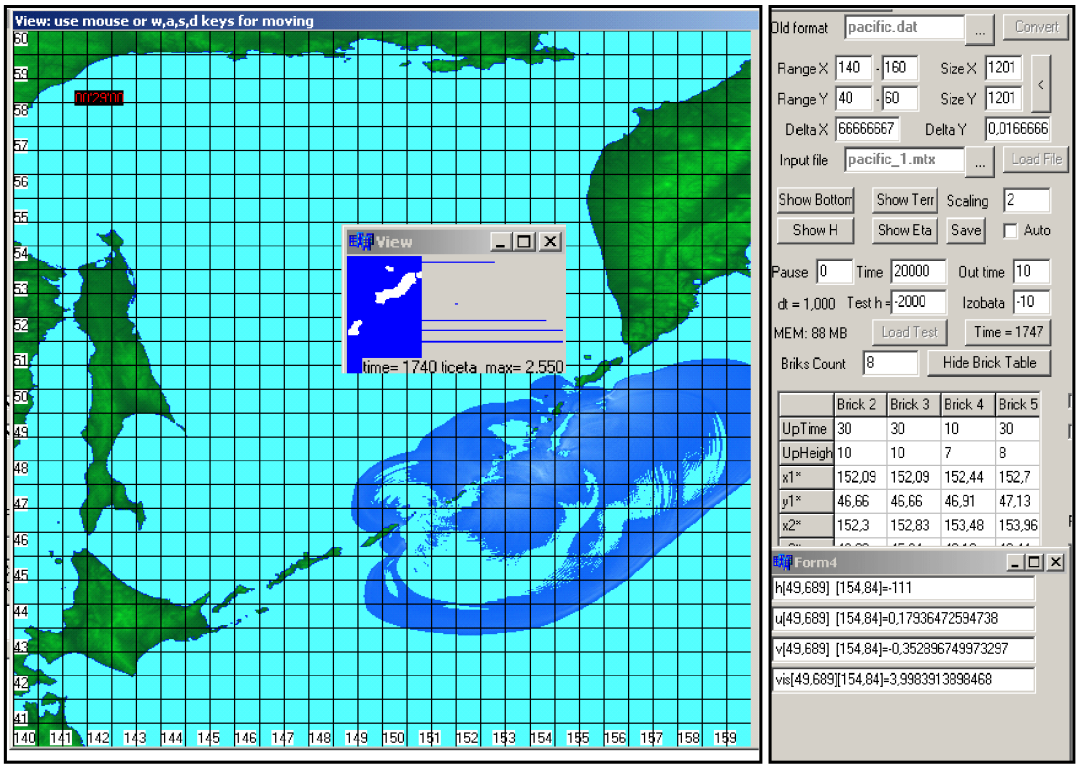


**Figure 4.** Interface of the program used for the generation and propagation of the tsunami wave excited by a complex keyboard source at the time moment $t = 29$ min measured from the wave generation onset time. The right-hand and middle insets show fragments of the control panel (see the text).

$$+\frac{1}{2\cdot\Delta y_{pj}}\left(v^n_{i+1j}\cdot\left(H^n_{i+2j}+H^n_{i+1j}\right)-v^n_{ij}\cdot\left(H^n_{i+1j}+H^n_{ij}\right)\right)\Big)\ .$$

[11] If a point lies in the moving region of the floor, the wave height is corrected for the increment with the appropriate sign. The velocities are then updated using the values of the wave height obtained in this way:

$$u^{n+1}_{ij}=u^n_{ij}-\frac{g\cdot\Delta t_j}{2\cdot\Delta x_p}\left(\eta^{n+1}_{ij}-\eta^{n+1}_{ij-1}\right)$$
$$-f\cdot v^n_{ij}-g\frac{u^n_{ij}\sqrt{u^{n^2}_{ij}+v^{n^2}_{ij}}}{Ch^2\left(H_{ij}+\eta^{n+1}_{ij}-B^{n+1}_{ij}\right)}\ ,$$

$$v^{n+1}_{ij}=v^n_{ij}-\frac{g\cdot\Delta t_j}{2\cdot\Delta y_{pj}}\left(\eta^{n+1}_{ij}-\eta^{n+1}_{i-1j}\right)$$
$$-f\cdot u^n_{ij}-g\frac{v^n_{ij}\sqrt{u^{n^2}_{ij}+v^{n^2}_{ij}}}{Ch^2\left(H_{ij}+\eta^{n+1}_{ij}-B^{n+1}_{ij}\right)}\ .$$

[12] Numerical calculations used the bathymetric map constructed by A. S. Svarichevsky (e.g. see [*Baranov et al.,* 1997; *Solovyev,* 1968]), with the isobath interval ranging from 100 m to 250 m. The calculations were performed in the square (40°–60°N, 140°–160°E) covered by a 1201×1201 grid. With the coordinate spacing being given, a time step optimal for the entire water area was found. Corrections for the Earth's curvature were introduced in the spacings (in meters) using the formulas

$$\Delta x_p=\frac{\Delta x\cdot\pi\cdot R_3}{180}$$

along meridians ($R_3$ is the Earth's radius) and

$$\Delta y_{p_j}=\frac{\Delta x_p\cdot\pi\cdot\cos(y_n+j\cdot\Delta y)}{180}$$

along parallels; the time step was found from the difference scheme stability condition,

$$\Delta t_j=\frac{\Delta x_p\cdot\Delta y_{pj}\cdot M}{\sqrt{g\cdot H_{\max}\cdot(\Delta x_p^2+\Delta y_{pj}^2)}}$$

, where $H_{\max}$ is the absolute value of the maximum depth in the water area considered and

$$M^2=\frac{1+\sqrt{f^2+1}}{2}\ .$$

[13] To describe free boundaries in the tsunami wave propagation problem, we chose the Sommerfeld condition, according to which the part of the wave field lying outside the boundary is transferred, without changing the waveform, in the direction of the outer normal with a constant velocity defined by the basin depth near the boundary. The software implementing the algorithms was compiled in the C++ language with the use of standard graphic programs.

## Brief Description of the Program Interface

[14] The brief description of the program interface (Figure 4) is exemplified by the calculation of the tsunami wave generation and propagation, with a seismic source consisting of

**Table 1.** Scenarios of the Tsunami Wave Generation for Three Blocks

| | Vertex coordinates of keyboard-blocks | | Variant 1 | | Variant 2 | | Variant 3 | |
|---|---|---|---|---|---|---|---|---|
| Block | E | N | Uplift height, m | Uplift time, s | Uplift height, m | Uplift time, s | Uplift height, m | Uplift time, s |
| 1 | 151°48′<br>152°36′<br>153°24′<br>154°00′ | 46°18′<br>46°00′<br>47°30′<br>47°06′ | 10 | 30; 30 | 10 | 30 | 10 | 30 |
| 2 | 153°24′<br>154°00′<br>154°18′<br>154°54′ | 47°30′<br>47°06′<br>48°15′<br>47°45′ | 10 | 30; 30 | 0 | 0 | 10 | 30 |
| 3 | 154°18′<br>154°54′<br>155°03′<br>155°42′ | 48°15′<br>47°45′<br>48°45′<br>48°18′ | 10 | 30; 60 | 10 | 30 | −10 | 30 |

eight keyboard-blocks (Figure 3). The tsunami source developing on the water surface is shown for the time moment $t = 25$ min from the onset of block motion in the seismic source. The fragment on the control panel presented in the right (Figure 4) shows the characteristic dimensions of the calculated region (40°–60°N, 140°–160°E), the number of grid nodes in this region (1201×1201), the chosen scale, the total computation time, the time required for drawing wave fronts, and the isobath for which the given calculation is carried out. Pressing the button "Show button", one can see the bathymetry of the desired part of the water area, while the button "Show H" shows the wave height distribution throughout the water area at the given time of computation. After the computation is terminated, the buttons "Show H" and "safe" allows one to fix the general pattern of the distribution of maximum heights throughout the water area up to the 10-m isobath along both continental and island coasts. Here is also a tableau showing the current time oceanic computations (in seconds). Parameters of the source are given below in the panel: the number of blocks and heights and times of their uplift (the parameters of only four blocks are shown in the figure). The following characteristics are shown in the right at the bottom of the panel: components of particle velocities on the water surface, the water depth, and a maximum height at a given point at the viewing time moment. All characteristics can be plotted in the real time mode at the request of the user. The inset at the center of the figure presents an example of the histogram for the given part of the basin (Onekotan and Paramushir islands). The histogram is constructed in the real time mode at the request of the user and presents maximum heights on the 10-m isobath along these islands at a given time moment. Additional blocks of the control panel are intended to plot the distribution of velocity characteristics throughout the wave propagation field, trace the wave front velocities in any directions, and obtain mareograms at any point of the water area, including offshore zones.

## Results of Numerical Simulation

[15] Two groups of calculations were performed in accordance with the two types of chosen seismic sources. In the first case, a model source 330 km in length and 70 km in width consisting of three 110-km-long blocks at a distance of 35 km from the Kurile Islands was considered (Figure 5a). The following scenarios of the tsunami wave generation were considered (Table 1):

[16] (1) Uplift of the three blocks by 10, 10, and 10 m over respective times of 30, 30, and 30 s and of 30, 30, and 60 s.

[17] (2) Simultaneous 10-m uplift of blocks 1 (in front of the Bussol Strait) and 3 (in front of the Kruzenshtern Strait) over 30 s, with block 2 being fixed.

[18] (3) Vertical block movements opposite in sign: blocks 1 and 2 are uplifted by 10 m over 30 s, and block 3 subsides by 10 m over 30 s.

[19] Movements in seismic source form a tsunami source. Our calculations show that, if vertical movements of blocks occur over a short time (10–30 s), the moving blocks act like a piston and, due to incompressibility of the liquid and hydrostatic pressure, the water surface is displaced (upward or downward) by the same value as the block in the seismic source. With a slower uplift of a blocks (over 60–120 s), the water surface displacement amounts to 70% or less of the seafloor block displacement, which is due to the relation between the horizontal and vertical velocities in the source during the block uplift. However, the forming tsunami source coincides in shape and sizes with the earthquake source [*Pelinovsky and Plink,* 1980; *Solovyev and Tulupov,* 1981], as is well seen in Figure 5. Figure 5a clearly displays the characteristic shape of tsunami sources formed at a time moment of the initial generation process for the scenario data presented in Table 1.

[20] The second group of calculations involved a more detailed source whose structure was defined by data gathered

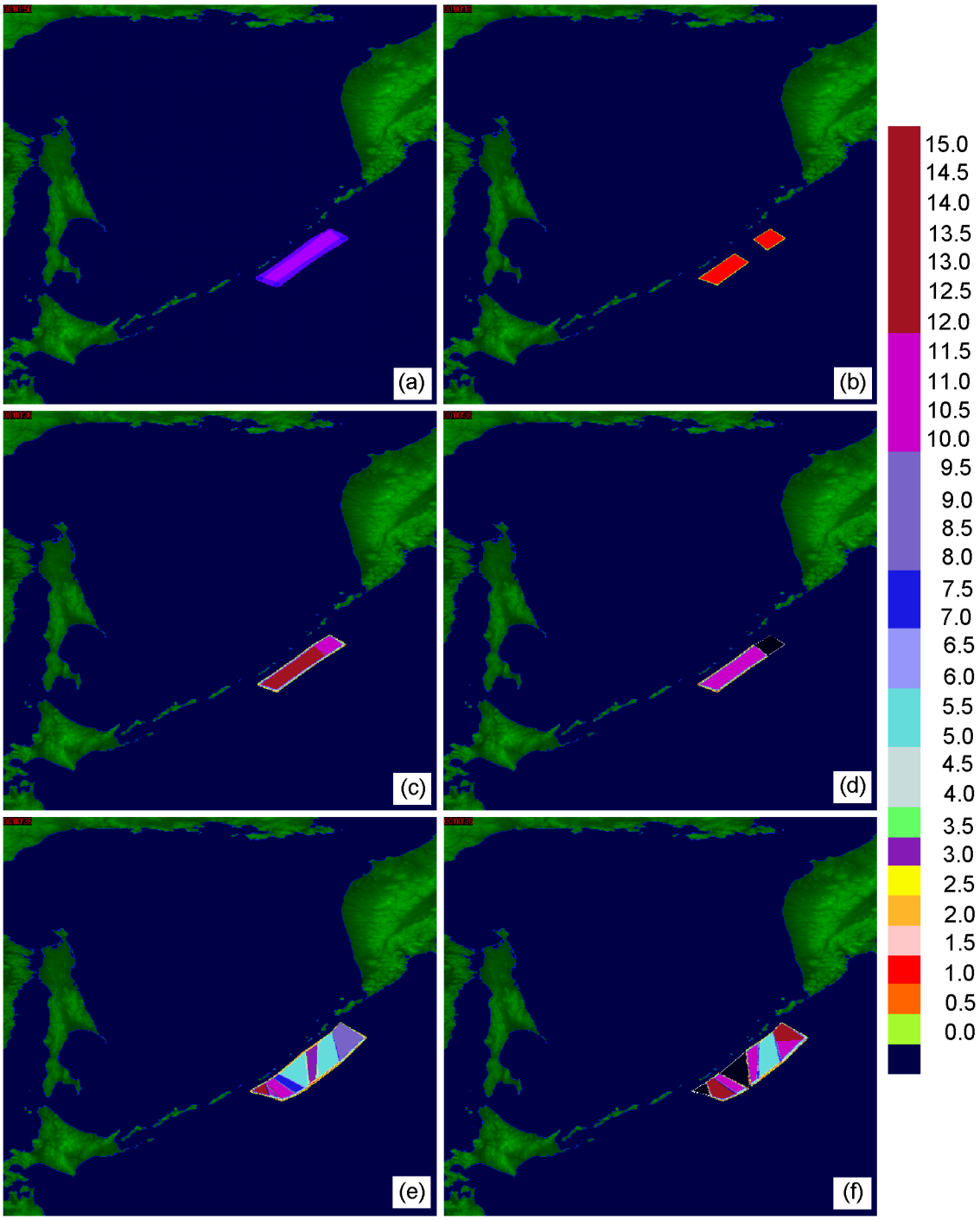


**Figure 5.** Variants used for the simulation of the dynamic tsunami source generation by a complex keyboard-block seismic source (Figure 3). (a) Three blocks: simultaneous uplift at the same velocities (left top panel); uplift of blocks 1 and 3 at the same velocities, with block 2 being fixed (right top panel); uplift of blocks 1–3 at different velocities (left middle panel); uplift of blocks 1 and 2 and subsidence of block 3, with all velocities being different (right middle panel). (b) Eight blocks: uplift of blocks 1–8 at different velocities (left bottom panel); uplift of blocks 2, 3, and 5–8 and subsidence of blocks 1 and 4, with all velocities being different (right bottom panel).

**Table 2.** Scenarios of the Tsunami Wave Generation for Eight Blocks

| | Vertex coordinates of keyboard-blocks | | Variant 1 | | Variant 2 | |
|---|---|---|---|---|---|---|
| Block no. | E | N | Uplift height, m | Uplift time, s | Uplift height, m | Uplift time, s |
| 1 | 151°26′<br>152°18′<br>152°05′<br>151°18′ | 46°15′<br>46°02′<br>46°40′<br>46°02′ | 14 | 10 | −10 | 10 |
| 2 | 152°05′<br>151°18′<br>151°05′<br>152°50′ | 46°40′<br>46°02′<br>46°40′<br>45°50′ | 10 | 30 | 14 | 30 |
| 3 | 152°05′<br>152°50′<br>152°26′<br>153°29′ | 46°40′<br>45°50′<br>46°55′<br>46°08′ | 10 | 30 | 14 | 30 |
| 4 | 152°26′<br>153°29′<br>152°42′<br>153°58′ | 46°55′<br>46°08′<br>47°08′<br>46°26′ | 7 | 10 | 10 | 10 |
| 5 | 152°42′<br>153°58′<br>153°55′<br>154°05′ | 47°08′<br>46°26′<br>48°15′<br>46°34′ | 8 | 30 | −8 | 30 |
| 6 | 153°55′<br>154°05′<br>154°29′<br>154°26′ | 46°26′<br>46°34′<br>48°41′<br>46°50′ | 10 | 10 | 10 | 10 |
| 7 | 154°29′<br>154°26′<br>155°11′<br>155°29′ | 48°41′<br>46°50′<br>49°13′<br>47°43′ | 5 | 30 | 5 | 30 |
| 8 | 155°11′<br>155°29′<br>155°31′<br>156°37′ | 49°13′<br>47°43′<br>49°40′<br>48°56′ | 10 | 10 | 10 | 10 |

from studies of the seismic gap zone (Figures 1 and 2). In this case, the source consists of eight keyboard-blocks reflecting the real position of crustal faults (Figure 2). The source is 465 km long and 130 km wide, and its distance to the Kurile Islands is 25 km. With this type of the source, two scenarios of tsunami generation were considered. The coordinates, uplift height, and uplift times of the blocks are presented in Table 2. The blocks can move both upward and downward. The realization of the given scenarios yielded the characteristic type of tsunami sources shown in Figure 5b for a time moment of the initial generation process.

[21] Computations according to each of these scenarios yielded displacement and velocity wave fields for the entire water area of the Sea of Okhotsk and for all coast of the continent and islands.

[22] Figures 6–8 present results of numerical simulation of the tsunami wave generation and propagation for a source consisting of three blocks (see Figure 5a and Table 1). Figure 6 illustrates the realization of scenario 2: the seismic source consists of two blocks in front of the Bussol and Kruzenshtern straits. Figure 6a presents the wave propagation patterns for 12 time moments: generation of the surface wave by the source (top panels), propagation of the wave crossing the Kurile island arc (middle panels), and propagation of tsunami waves throughout the water area of the Sea of Okhotsk (bottom panels). Figure 6b shows the distribution of calculated maximum heights in the entire water area of the Sea of Okhotsk.

[23] Figure 7 presents results of numerical simulation of the tsunami wave generation and propagation realizing sce-

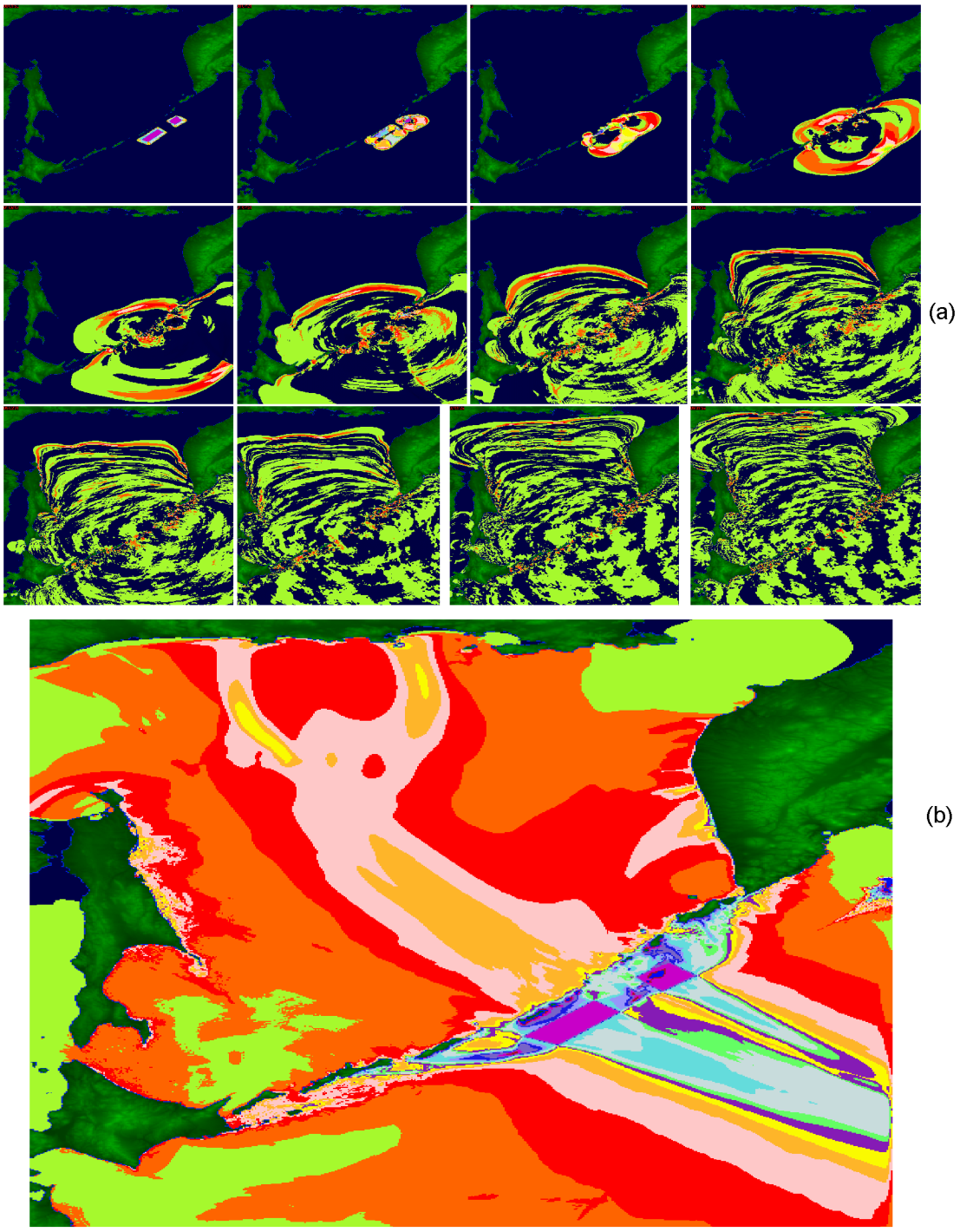


**Figure 6.** Generation and propagation of the tsunami wave in the Sea of Okhotsk water area; the wave is generated in the seismic gap zone of the central Kurile Islands by a source consisting of two seafloor blocks simultaneously uplifted by 10 m over 30 s (left top panel). (a) Position of the wave front at 12 successive time moments. (b) Distribution of wave heights in the water area, with maximum heights along the eastern Sakhalin coastline varying from 1.5 m to 5.5 m.

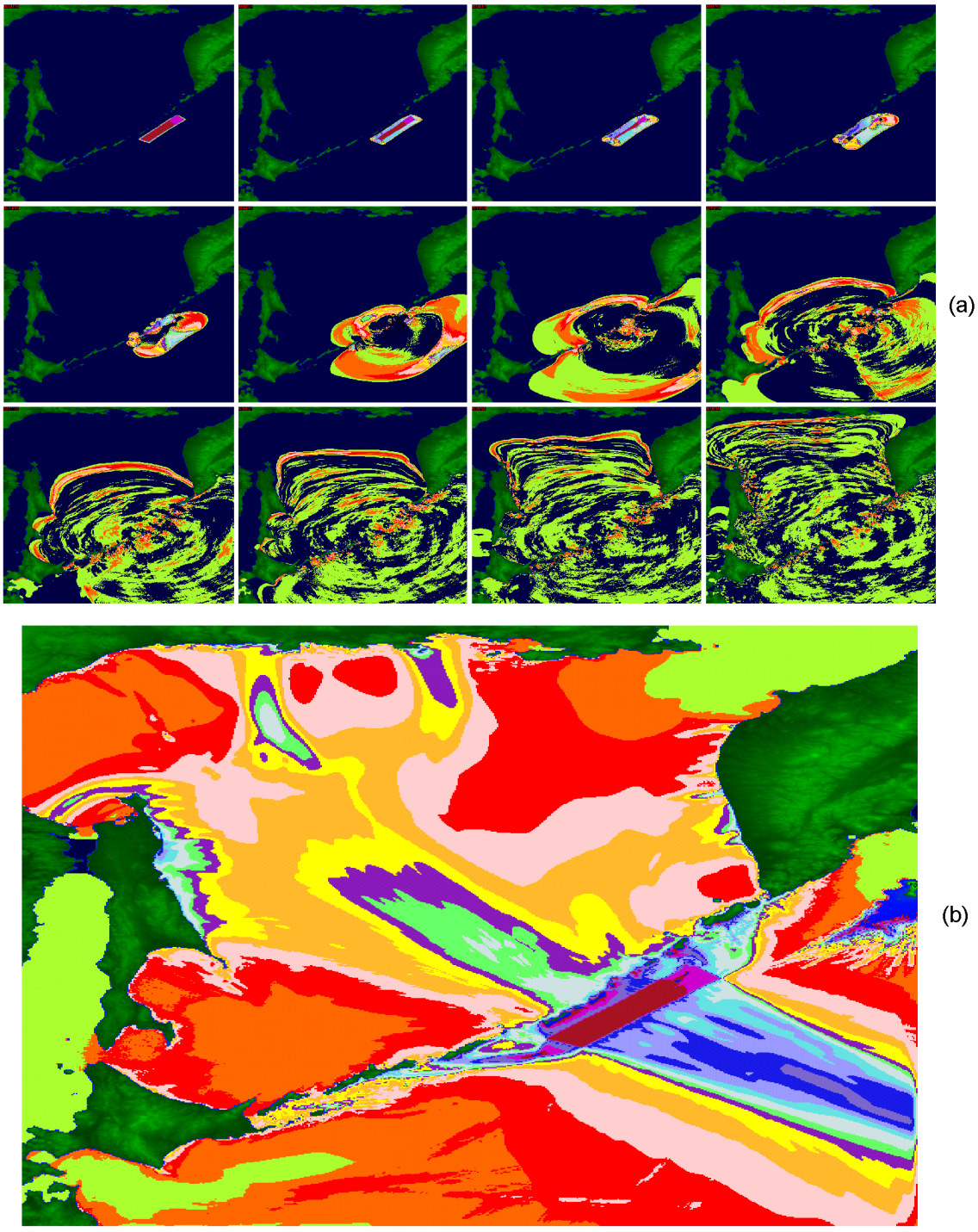


**Figure 7.** Generation and propagation of the tsunami wave in the Sea of Okhotsk water area; the wave is generated in the seismic gap zone of the central Kurile Islands by a source consisting of three seafloor blocks, two of which are uplifted by 10 m over 30 s and the third block is uplifted by 10 m over 60 s. (a) Position of the wave front at 12 successive time moments. (b) Distribution of wave heights in the Sea of Okhotsk water area, with the maximum height along the eastern Sakhalin coastline attaining 7 m.

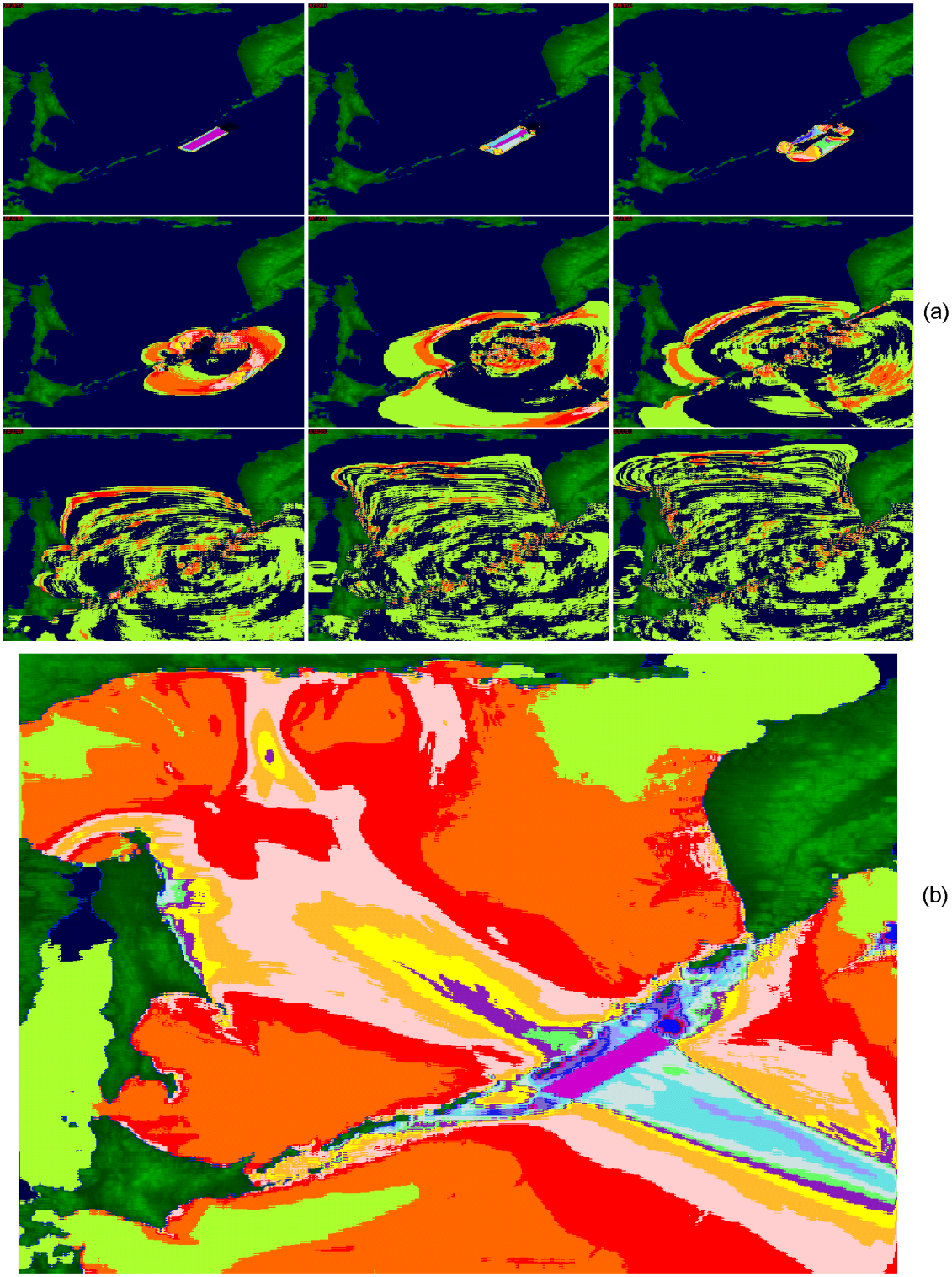


**Figure 8.** (a) Generation and propagation of the tsunami wave in the Sea of Okhotsk water area; the wave is generated in the area of central Kurile Islands by a source consisting of three seafloor blocks: blocks 1 and 2 are simultaneously uplifted by 10 m over 30 s and block 3 is subsided by 10 m over 30 s. (b) Distribution of wave heights in the water area, with the maximum height along the eastern Sakhalin coastline reaching 7 m.

nario 3, with a seismic source consisting of three blocks two of which are displaced upward by 10 m over 30 s, while the third moves upward for the same distance more slowly, over 60 s. Figure 7a presents the wave propagation patterns for 12 time moments: generation of a surface wave by the source (top panels), propagation of the wave crossing the Kurile island arc (middle panels), and propagation of tsunami waves throughout the water area of the Sea of Okhotsk (bottom panels). Figure 7b shows the distribution of the calculated maximum heights over the entire water area under consideration.

[24] Figure 8 displays results of numerical simulation of the tsunami wave generation and propagation realizing scenario 4 (the seismic source consists of three blocks two of which are displaced upward by 10 m over 30 s and the third block is displaced downward by 10 m over 30 s). Figure 8a presents the wave propagation patterns for nine time moments: generation of a surface wave by the source (top panels), propagation of the wave crossing the Kurile island arc (middle panels), and propagation of tsunami waves throughout the water area of the Sea of Okhotsk (bottom panels). Figure 8b shows the distribution of the calculated maximum heights over the entire water area under consideration.

[25] As seen from Figures 6–8, the movement of the tsunami wave across the Kurile Islands and propagation both outside and inside the water area of the Sea of Okhotsk follow nearly the same pattern: in the first 150–240 s, a part of the wave goes away into open ocean, toward the Hawaiian Islands. On the other hand, the Vityaz Ridge and the Kurile Islands hinder the propagation of the wave toward the Sea of Okhotsk, thereby increasing the height of the wave run-up at SE coasts of the islands (up to 15 m on Simushir Island, 2 m on Kunashir Island, 1.5 m on Shikotan Island, and so on). Some part of the wave energy is reflected by the islands toward the ocean, but the main part of the wave moves through the Bussol and Kruzenshtern deep straits, which play the role of natural waveguides.

[26] The further propagation of the wave is largely controlled by the bathymetry of the water area: a part of the wave that passed through the Bussol Strait propagates along the Kurile trench toward Sakhalin and Hokkaido islands at a relatively high velocity ($v \sim 600$ km h$^{-1}$) due to a considerable depth of this trench ($H \sim 3500$ m). The velocity of the second wave, passing through the Kruzenshtern Strait and moving across the Kurile trench appreciably decreases with time, as the wave reaches the significantly shallower Deryugin trough.

[27] After 50–70 minutes, the joint front of waves that propagated through the Bussol and Kruzenshtern straits reaches the SE termination of Sakhalin Island (the Terpeniya Promontory). As is evident from the modeling results, the run-up onto the eastern coast of Sakhalin Island is first produced by the wave that passed through the Kruzenshtern Strait. As the wave propagates toward the continental Sea of Okhotsk coast, the left part of the wave front successively (from south to north) strikes the eastern Sakhalin coast. The run-up heights of this wave range from 2.5 m to 7 m, depending on the scenario considered. After leaving Sakhalin, the wave front becomes nearly plane-shaped and propagates at a relatively low velocity toward the town of Okhotsk, while the flank fronts move at a higher velocity westward the Shantarksie Islands and eastward toward the Shelikhov Bay and reaches the continental coast in about three hours, depending on the scenario considered (bottom panels in Figures 6a–8a). Although the wave propagation patterns determined from the first group of calculations are similar, the detailed distributions of maximum wave heights along all coasts of the water area under study (particularly, along the Sakhalin coast) differ significantly, as is clearly seen from Figures 6b–8b.

[28] The results obtained for two scenarios of the first type (the seismic source is specified by three blocks) are compared in Figure 9. Figure 9a presents the distribution of heights over the entire water area of the Sea of Okhotsk for the case when the source blocks are simultaneously displaced by 9 m upward over 30 s. Figure 9b shows the distribution of heights for the case when the blocks are displaced upward by 12, 10, and 12 m over 10, 30, and 10 s, respectively. As is well seen the distributions of heights in these two cases are somewhat different. Along the Sakhalin coast, they can differ by 1.5 to 2 times. The insets in the figure present mareograms for the point (52.2°N, 143.6°E). It is clearly seen that the maximum height in the second case (3 m) is twice as high as in the first case (1.5 m).

[29] Figures 10 and 11 present the results of numerical simulation of the tsunami wave generation and propagation obtained from calculations of the second series for a seismic source consisting of eight blocks (see Figure 5b and Table 2). Figure 10a shows the wave propagation patterns for 12 time moments: generation of a surface water wave by the source (top panels), propagation of the wave crossing the Kurile island arc (middle panels), and propagation of tsunami waves throughout the water area of the Sea of Okhotsk (bottom panels). Figures 10 and 11 show that, as compared with the case illustrated in Figures 6–8, the change in the structure of the source and its sizes has the most significant effect on the near-field zone, i.e. on the distribution of run-up heights on the nearest Kurile islands (see Figures 10b and 11b). After the passage of the wave through the Bussol and Kruzenshtern straits, the wave front becomes more indented compared to the case of a three-block source (Figures 6–8). Moreover, in the latter case, a nearly quiet water surface is observed in the Sea of Okhotsk water area behind the wave train moving from the source after the passage of these straits whereas, in the case of an eight-block source, the tsunami propagating in the Sea of Okhotsk yield a distinct wave pattern observed up to the Kurile Islands, particularly well expressed in the case when two of eight keyboard-blocks in the source move downward (Figure 11). Such a structure of the wave field in the water area leads in turn to changes in the arrival times of the wave front at points of the Sea of Okhotsk coastline and in the inundation shape and run-up values. Figures 10b and 11b shows the distribution of maximum wave heights over the entire water area under study obtained from the computations of the given series.

[30] The distributions of velocity fields for scenario 2 from the second series of calculations (Table 2) are presented in Figure 12. The left panel displays the waveform in the dynamic source of tsunami during the generation of the wave by a seismic source of the keyboard-block type at the time

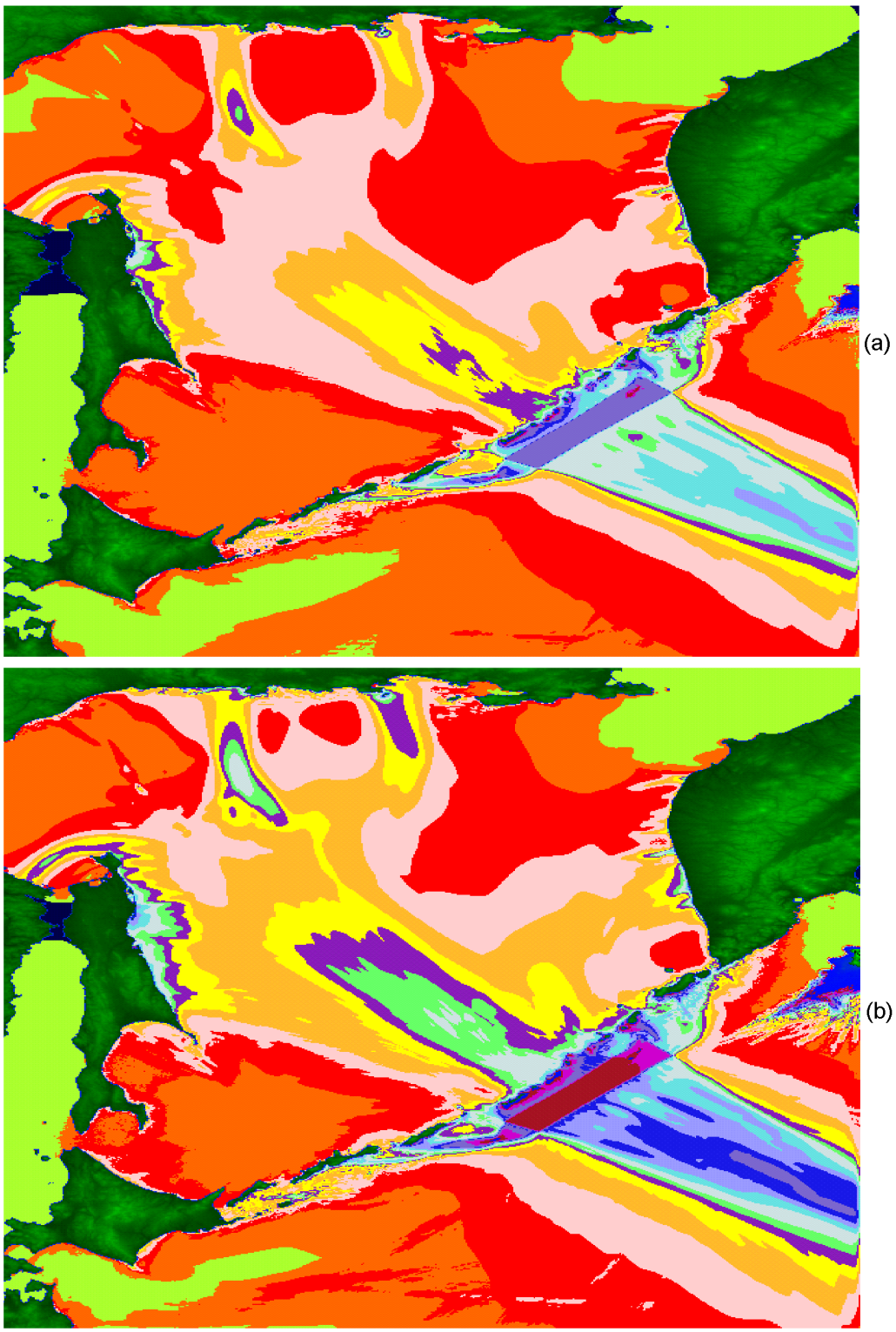


**Figure 9.** Distribution of wave heights along Sea of Okhotsk coastlines; the tsunami waves are generated by a seismic source consisting of three blocks (Figure 3): (a) all blocks move simultaneously upward for 9 m over 30 s; (b) blocks 1, 2, and 3 are uplifted by 12, 10 et al. and 12 m over 10, 30, and 10 s, respectively. The maximum wave height along the Sakhalin coastline is 5 m in the first case and 7 m in the second case. The inset shows mareograms at the point (52.2°N, 143.6°E).

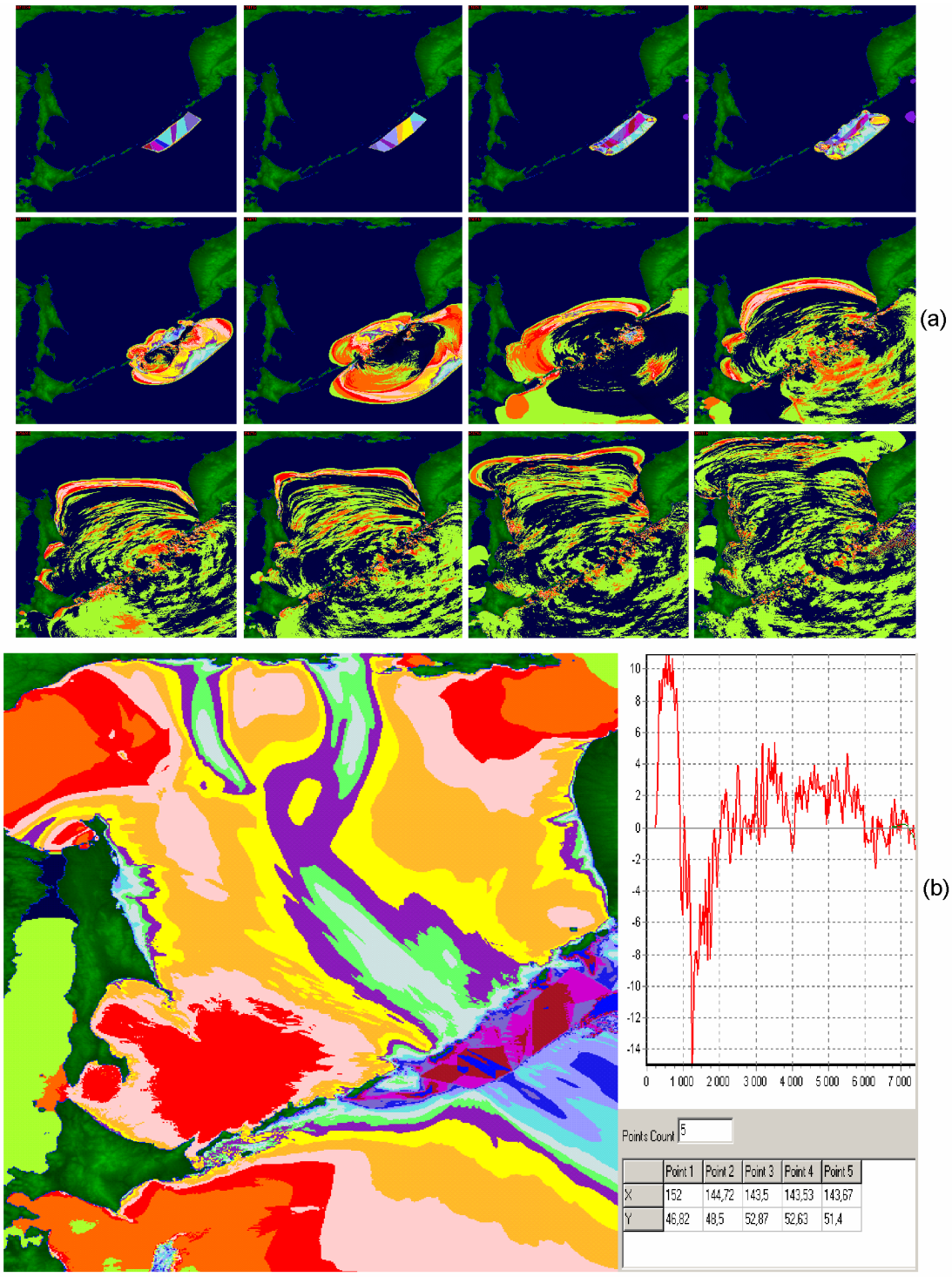


**Figure 10.** (a) Generation and propagation of the tsunami wave in the Sea of Okhotsk water area; the wave is generated in the area of the central Kurile Islands by a source consisting of eight blocks (Figure 3): blocks 1–8 are uplifted by 14, 10, 10, 14, 9, 9, 12, and 9 m over 10, 10, 10, 30, 10, 30, 30, and 10 s, respectively. (b) Distribution of wave heights in the Sea of Okhotsk water area, with the maximum run-up along the eastern Sakhalin coastline reaching 8 m.

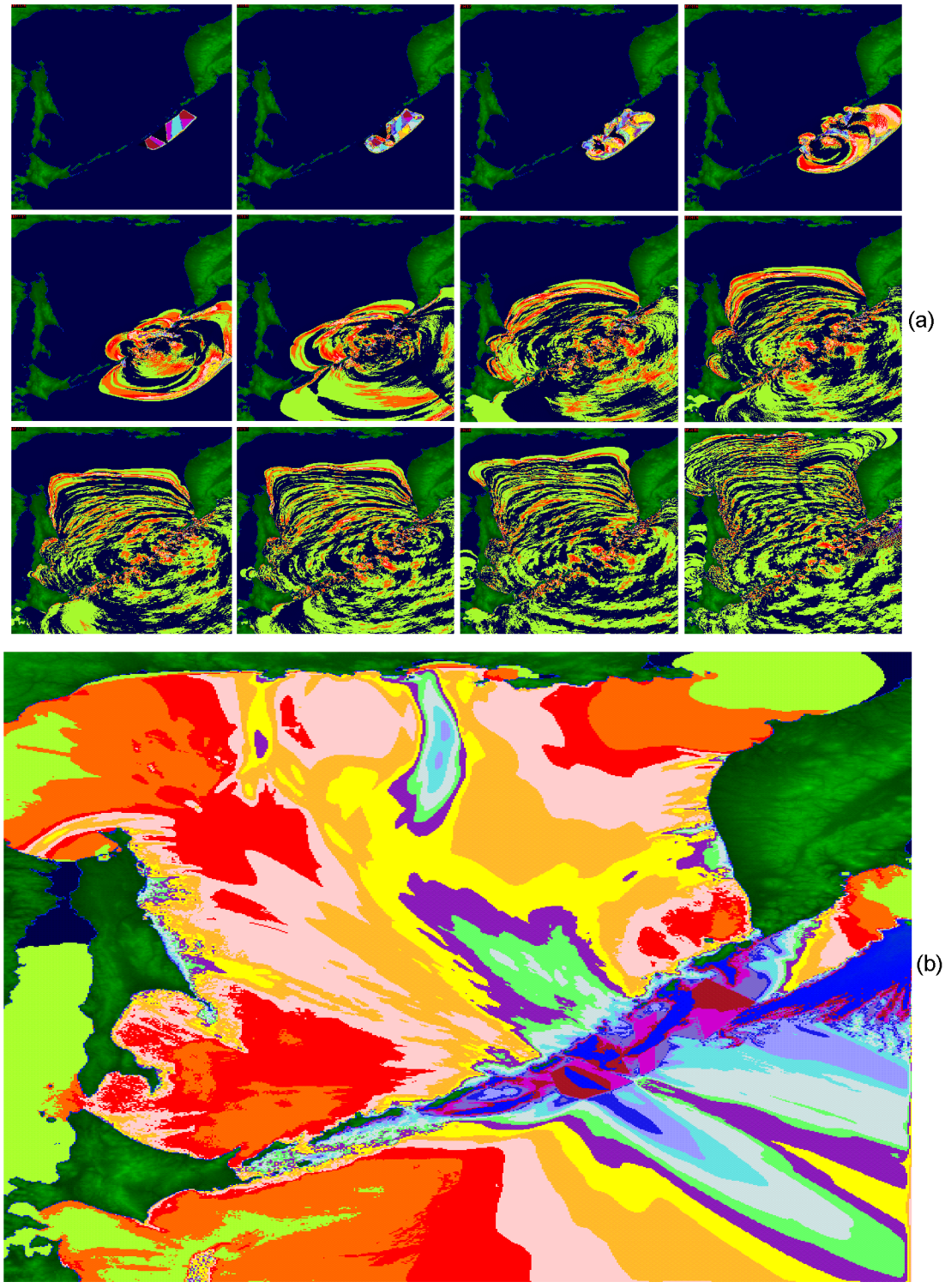


**Figure 11.** (a) Generation and propagation of the tsunami wave in the Sea of Okhotsk water area; the wave is generated by a source consisting of eight blocks (Figure 3): blocks 1–8 move vertically for 10, 14, 14, 10, 8, 10, 5, and 10 m over 10, 10, 10, 30, 10, 30, 30, and 10 s, respectively. (b) Distribution of maximum wave heights, with the maximum run-up along the eastern Sakhalin coastline reaching 5 m.

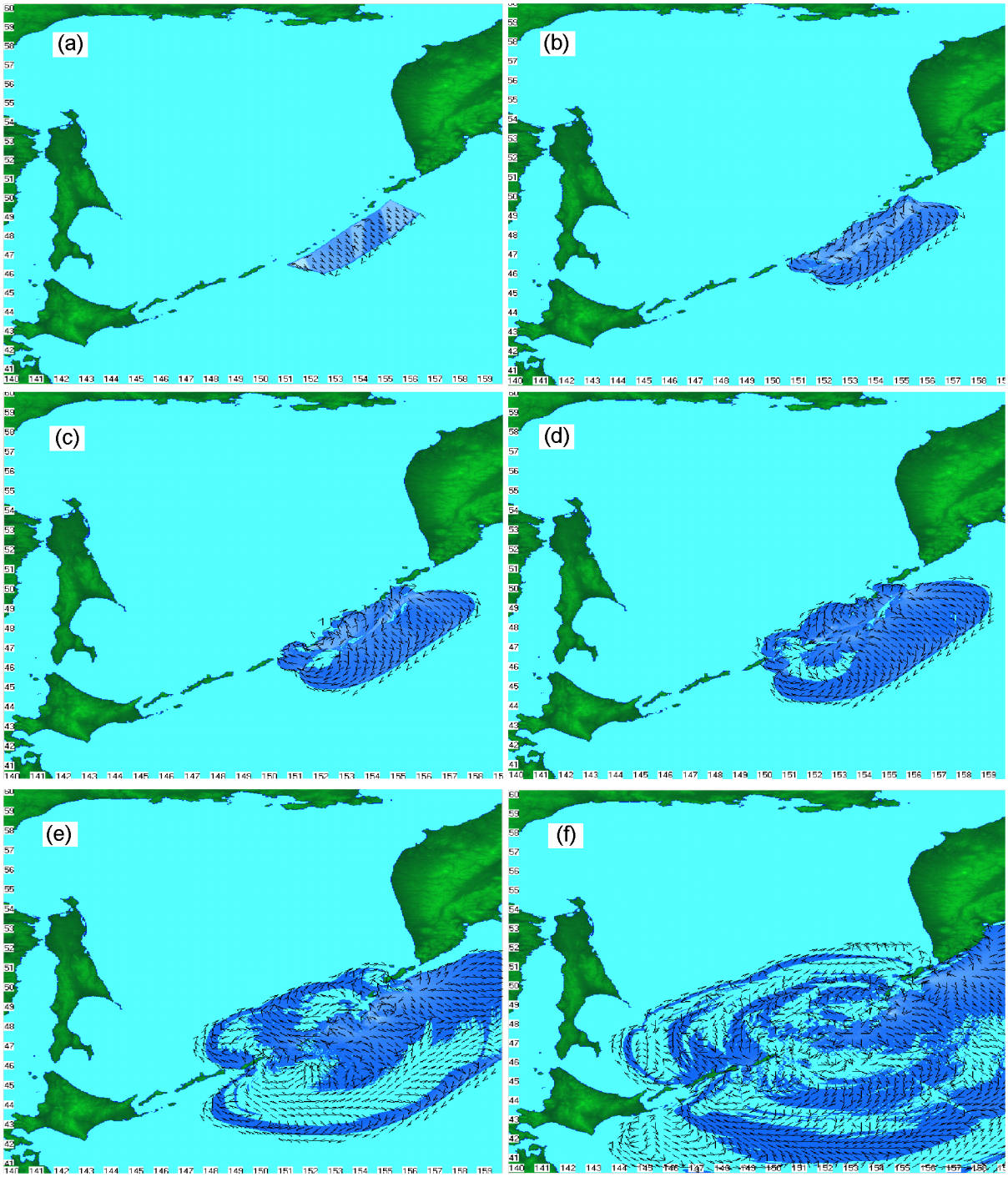


**Figure 12.** The velocity field of water particles at six characteristic time moments (measured from the onset time of the wave generation by a seismic source): $t$ = 20 s, 6 min, 11 min, 19 min, 39 min, and 1 h 16 min.

moment $t$ = 20 s. By this time, keyboard blocks 1, 4, 6, and 8 stopped moving, while blocks 2, 3, 5, and 7 continue to move upward at the given velocities (see Table 2).

[31] The field of water particle velocities (shown by arrows) in the tsunami dynamic source region is largely controlled by both bathymetric details of the trench slope and movement parameters of blocks (their heights and velocities). Since the keyboard-blocks are located on the NW slope of the deep-sea trench, a feature typical of the entire area of the dynamic tsunami source is the movement of water from the left, up-

lifted edge of the source in the SE direction toward the right, farther from the island arc, source boundary, along which a depression arises. Water particles at the right-hand source boundary move along it, mainly in the SW direction. The movement in the vicinity of the lower point of the contact between blocks 6 and 7 is of the eddy type, which is apparently due to differences between the uplift heights of the blocks at the given time moment and between the velocities of their vertical motions. A local elevation of surface water is observed above the lower part of the boundary between blocks 4 and 5, while the bulk of water moves away from block 4; this is likely due to the further uplift of block 5, after block 4 stops moving. Vortex motion also arises in the source region corresponding to the upper contact between blocks 5 and 6, which might be accounted for by the continuing uplift of block 5, while the water rise due to the uplift of block 6 is already developed.

[32] The right-hand top panel displays the wave field generated by the given seismic source at the time when the left flank of the wave front formed in the process of tsunami generation reached the Kurile Islands, while the right flank of the front continues to move into the open ocean toward the Hawaiian Islands ($t = 300$ s $\gg T$, where $T$ is the maximum time of the uplift of blocks); the right front remains linear nearly all along its extent, while the left front becomes strongly indented. The field of water particle velocities (shown by arrows) has an eddy pattern almost in the entire region of disturbed water surface. The wave field to the right of trench axis is dominated by the motion of water particles in the SW direction (along the right-hand front). On the contrary, the part of the wave field between the trench axis and the island arc is dominated by particle motion in the NE direction (along the island arc). Moreover, notwithstanding the large observation time ($t = 300$ s $\gg T$), the wave field still reflects the distribution of maximum heights (in the areas of blocks 1–3, 6, and 8). Water particles near the wave front move along the front line.

[33] The left middle panel presents the wave field at the time moment $t = 670$ s. While the right-hand linear front continues to move farther into the ocean toward the Hawaiian Islands, the left-hand part of the wave, after passing through the Kruzenshtern and Bussol deep straits, penetrated into the water area of the Sea of Okhotsk in the form of two, still separate wave fronts. Although the distribution of water particle velocities remains to be of the eddy type, dynamics of the wave process leads to a self-consistent motion of water particles along the normal to the wave front; near the wave front, this motion becomes directed along the front. In the left part of the wave moving into the Sea of Okhotsk, water particle velocities are directed toward the Kruzenshtern and Bussol straits, along the normal to the wave fronts forming after the waves leave the straits. Such behavior of the water particle velocities indicates that a water rise responsible for such a motion forms in the trench axis zone.

[34] The right-hand middle panel presents the wave field at the time moment $t = 1150$ s. Whereas the water particle velocity field is still homogeneous in the right-hand part of the wave, particles in the left-hand part move in a complex way. The wave fronts from both straits joined by this time, and the tsunami wave with the general wave front propagates across the water area of the Sea of Okhotsk. The velocities are directed away from the source arising at the center of the wave field.

[35] The left-hand bottom panel shows the wave front at the time moment $t = 2340$ s. The situation is different compared to the previous time moment: a crest formed at the right-hand front; outside this crest (in the trough), the water particle velocities are parallel to the wave front and particles move in the SW direction. This area is followed by a zone where the particle velocities, also being parallel to the front, move in the opposite (NE) direction. In the left part of the wave, the joint wave front continues to travel across the Sea of Okhotsk, approaching Sakhalin Island.

[36] The right-hand bottom panel displays the wave field at the time moment $t = 4560$ s. Here the wave pattern characteristic of the far-field zone of the tsunami propagation is already formed: alternating crests and troughs are observed within the wave front.

## Detailed Analysis of Possible Catastrophic Tsunamis on the Kurile Islands

[37] To analyze possible catastrophic earthquakes in this region that can generate an anomalously strong tsunami along coastlines of the Kurile Islands, we performed the following calculations, assuming that the velocity of blocks and their displacement are fixed. The succession and direction of movements of blocks were varied in the modeling calculations. We considered a source consisting of three blocks (Figure 3) and analyzed the following scenarios of block movements in the source (Figure 13):

**(a)** uplift of the three blocks by 10, 8, and 10 m over respective times of 30, 10, and 30 s (Figure 13a);

**(b)** uplift of the first and third blocks by 10 m and subsidence of the second block by 8 m; the respective motion times of the blocks are 30, 10, and 30 s (Figure 13b);

**(c)** uplift of the first and second blocks by 10 and 8 m and subsidence of the third block by 10 m; the respective motion times of the blocks are 30, 10, and 30 s (Figure 13c);

**(d)** uplift of the second block by 8 m and subsidence of the first and third blocks by 10 m; the respective motion times of the blocks are 30, 10, and 30 s (Figure 13d).

In realizing these scenarios, all blocks start moving simultaneously.

[38] Figure 14 presents the distributions of maximum wave heights in the calculated region. As is clearly seen, these distributions differ significantly depending on the type of the earthquake source. Results of the calculations are presented in Table 3.

[39] The histograms of maximum tsunami wave heights along coastlines of the Kurile Islands are shown in Figure 15

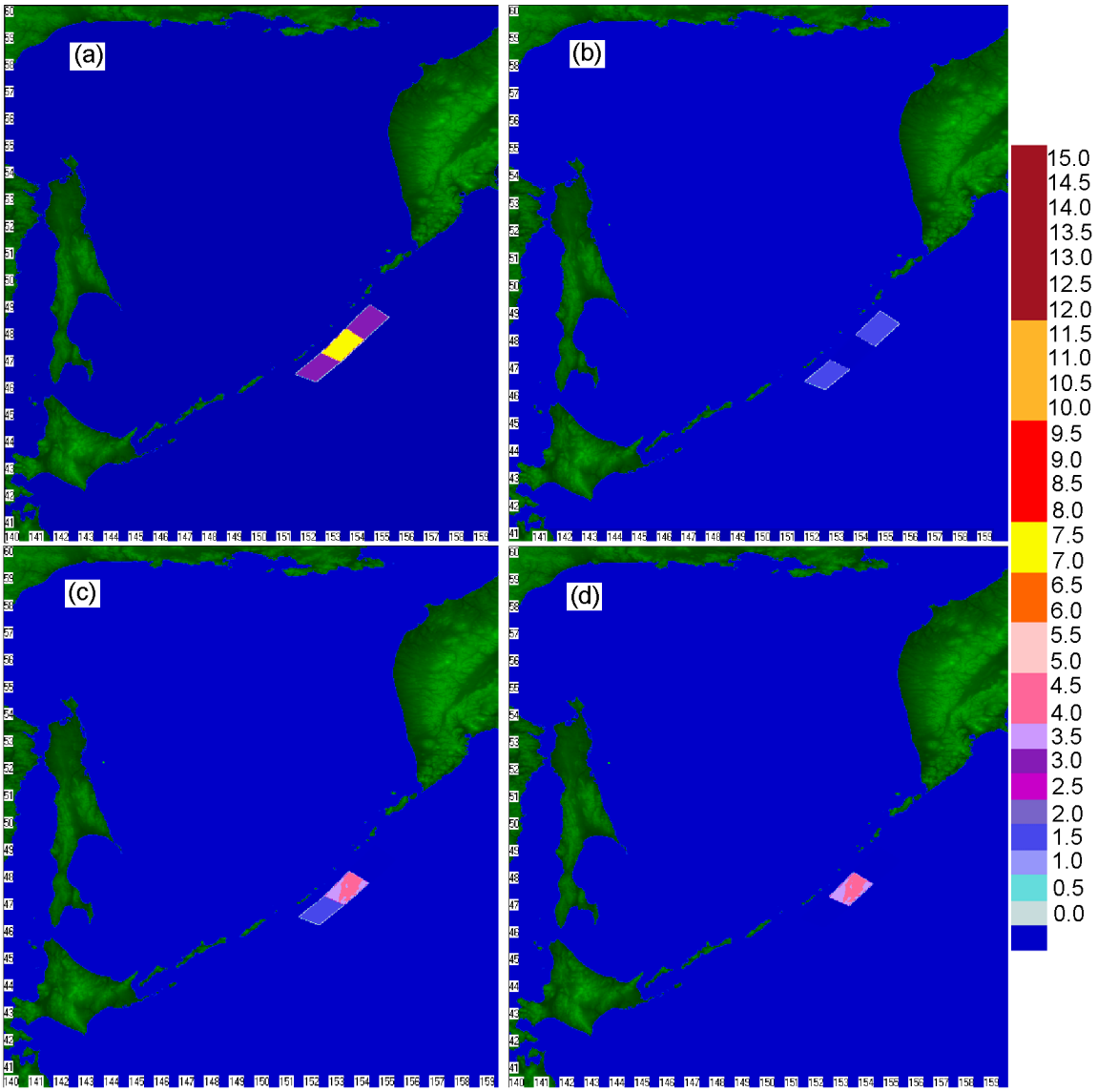


**Figure 13.** Simulation variants of the tsunami source generation by a seismic source consisting of three blocks: (a) simultaneous uplift of all blocks; (b) uplift of two left and right blocks and subsidence of the middle block; (c) uplift of the left and middle blocks and subsidence of the right block; (d) uplift of the middle block and subsidence of the two other block. Upward and downward movements of blocks occur at different velocities.

(left panels) for various types of a seismic source (Figure 13). The right-hand panels of Figure 15 show the position of points on coastlines of Iturup, Urup, Simushir, Onekotan, and Paramushir islands where the wave heights reach maximum values. It is well seen that, depending on the calculated variant, maximum values of the run-up height are attained at points separated by rather great distances. For example, the Urup island maximum run-ups are attained at the following coastline points for the variants shown in Figures 13a–13d: (45°32′ N, 149°26′ E), ∼9 m (Figure 13a); (46°10′ N, 150°30′ E), 8 m (13b); (45°54′ N, 150°8′ E), 7 m (13c); and (45°35′ N, 149°43′ E), 14 m (13d).

[40] The analysis of the considered scenarios of the keyboard-block movements in a seismic source (Figures 5 and 13) provided estimates of maximum wave heights along Pacific and Sea of Okhotsk coastlines of the Kurile Islands and the Kamchatka Peninsula (Table 3 (c)). It is clearly seen that, for any variant of block motions in the seismic source, the Sea of Okhotsk coast of the islands experiences a fairly weak impact, the largest predicted heights of waves being no more than 2.5 m. An exception is Urup, Simushir, and Shiashkotan islands where large wave heights are possible not only at the Pacific coast (more than 15 m) but also along coastlines of the Sea of Okhotsk (up to 7 m). On the

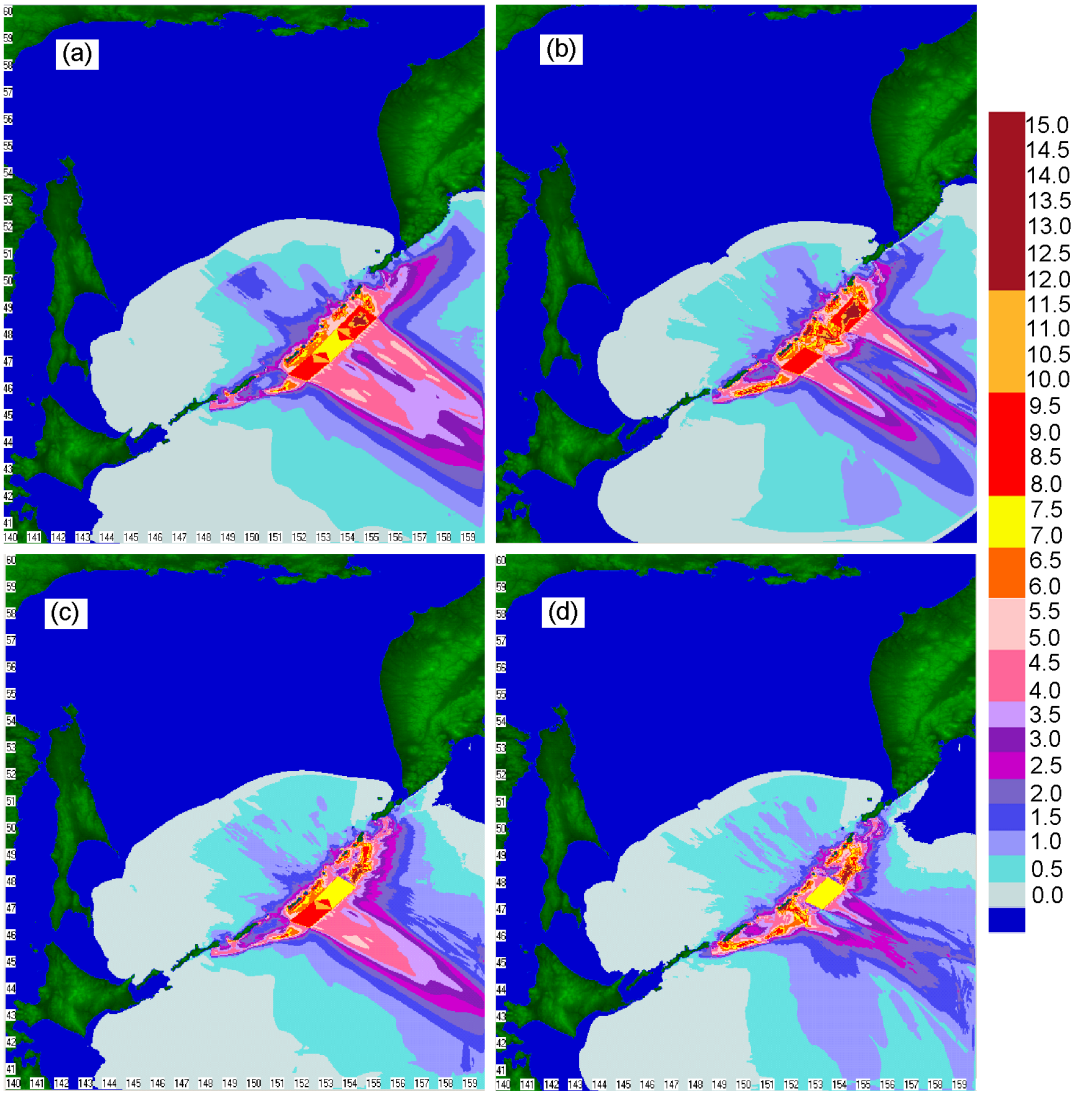


**Figure 14.** Distribution of tsunami wave heights in the region of calculations.

**Table 3.** Maximum Wave Heights in the Calculated Region

| Variant | | Islands | | | | |
|---|---|---|---|---|---|---|
| | | Iturup | Urup | Simushir | Onekotan | Paramushir |
| **(a)** | Coordinates of the point | 147°8′<br>44°30′ | 149°26′<br>45°32′ | 152°18′<br>47°6′ | 154°38′<br>49°14′ | 155°24′<br>50°1′ |
| | Maximum height, m | 8.79 | 8.61 | 15.2 | 8.87 | 5.54 |
| **(b)** | Coordinates of the point | 148°23′<br>45°12′ | 150°30′<br>46°10′ | 151°52′<br>46°49′ | 154°58′<br>49°40′ | 155°35′<br>50°9′ |
| | Maximum height, m | 6.16 | 7.62 | 14.64 | 15.1 | 3.43 |
| **(c)** | Coordinates of the point | 147°36′<br>44°52′ | 150°8′<br>45°54′ | 152°10′<br>46°60′ | 154°47′<br>49°14′ | 156°6′<br>50°26′ |
| | Maximum height, m | 5.21 | 7.38 | 13.78 | 13.78 | 4.60 |
| **(d)** | Coordinates of the point | 148°48′<br>45°20′ | 149°43′<br>45°35′ | 151°59′<br>46°50′ | 154°50′<br>49°30′ | 155°11′<br>50°11′ |
| | Maximum height, m | 6.05 | 14 | 15.3 | 11.29 | 6.58 |

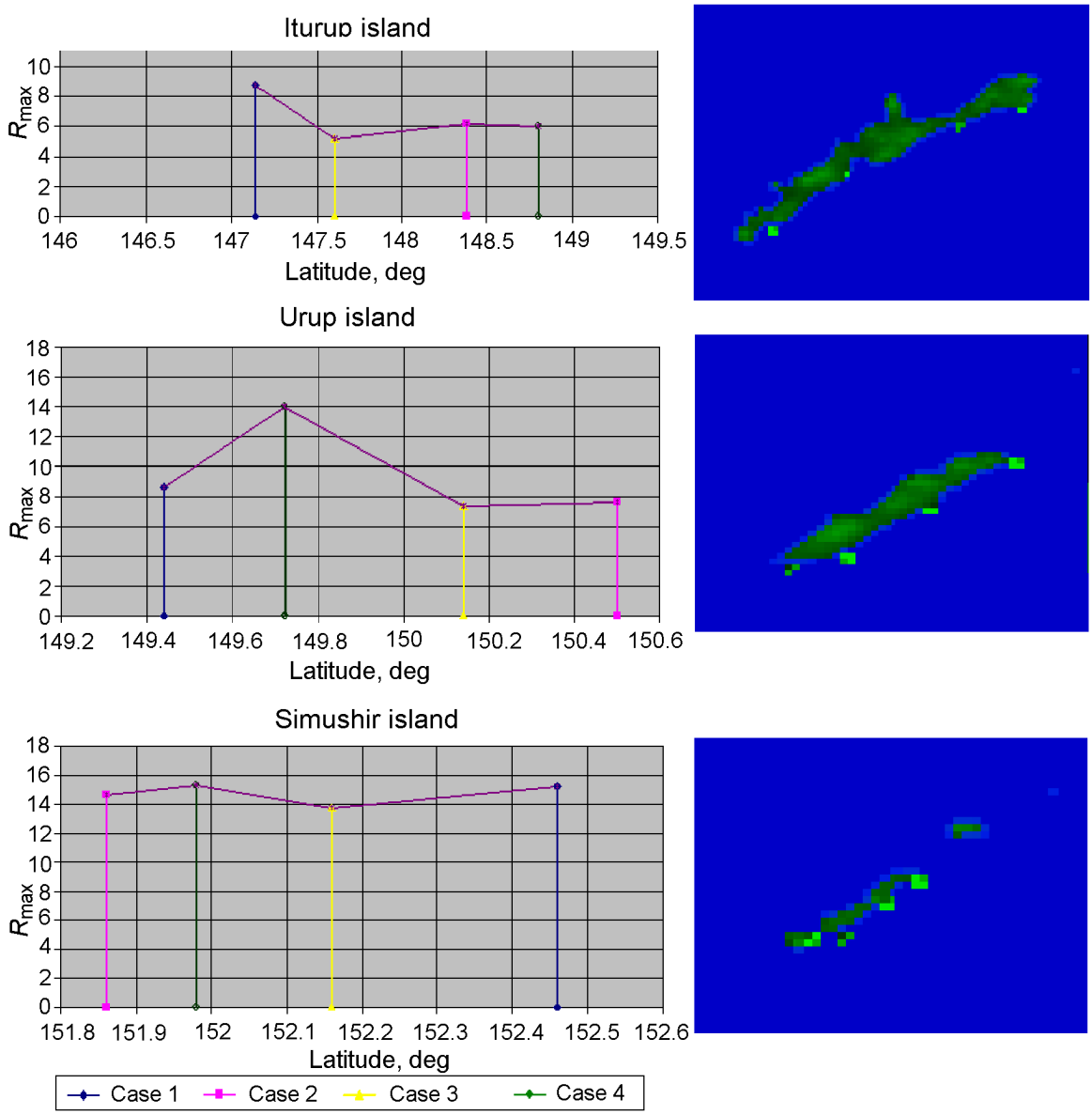


**Figure 15.** Maximum tsunami wave heights along coastlines of the Kurile Islands for various types of a seismic source. The histogram of wave heights versus the latitudes of coastline points is shown on the left. The distribution of maximum wave height points on the island coastline is shown on the right.

Kamchatka Peninsula, the wave heights reach 4.5 m along the Pacific coastline and 6 m along the Sea of Okhotsk coastline. Table 4 presents a summary of maximum possible wave heights along the Sea of Okhotsk and Pacific coastlines of the Kurile Islands obtained from calculations of all scenarios under consideration.

### Estimates of Tsunami Run-up Values on Sakhalin Island

[41] In the numerical simulation of the tsunami wave and estimation of wave heights along coastline, these values are generally determined at a certain distance from the coastline for a fixed depth (e.g. for a 10-, 20-, or 30-m isobath). Depending on the geometry of the coastal zone, this ensures an adequate accuracy for estimating the possible catastrophic damage on coast. However, to obtain more accurate estimates, detailed calculations of the tsunami run-up along a coastline are required with due regard for the complex topography of the coastal zone, but this is not always possible due to lacking detailed offshore bathymetric data or inadequate technical capabilities. Nevertheless, the run-up calculation is not methodologically difficult for concrete coastal points. In this work we obtained, as an example, run-up estimates for four points of the Sakhalin coastline at latitudes

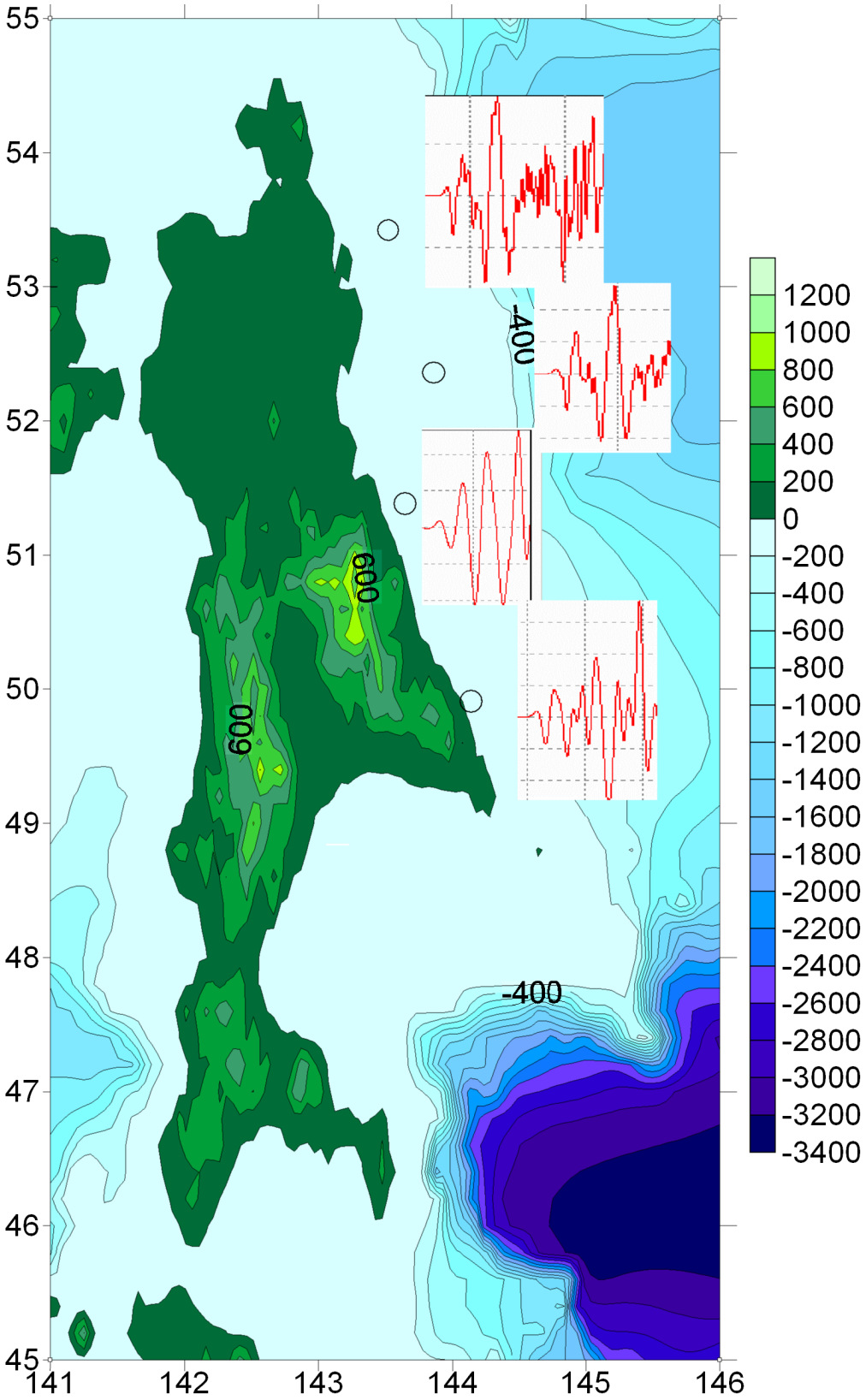


**Figure 16.** Schematic illustration of four cases of calculating the tsunami wave run-up along the Sakhalin coastline. The red line shows the form of the first wave in the wave train arriving at the coast. The circles mark the initial positions of the wave whose parameters were used for the calculation.

**Table 4.** Summary of Maximum Possible Wave Heights

| Island | Coast | Maximum wave height, m |
|---|---|---|
| Urup | Pacific | 15 |
| | Sea of Okhotsk | 3.9 |
| Simushir | Pacific | 15.3 |
| | Sea of Okhotsk | 6.7 |
| Shiashkotan | Pacific | 10.6 |
| | Sea of Okhotsk | 5 |
| Onekotan | Pacific | 15.1 |
| | Sea of Okhotsk | 2.55 |
| Paramushir | Pacific | 6.8 |
| | Sea of Okhotsk | 2.5 |
| Shikotan | Pacific | 1.91 |
| | Sea of Okhotsk | 0.8 |
| Iturup | Pacific | 9.2 |
| | Sea of Okhotsk | 2 |
| Shumshu | Pacific | 3.7 |
| | Sea of Okhotsk | 1.5 |
| Kamchatka | Pacific | 5.5 |
| | Sea of Okhotsk | 2.5 |

of 50°00′, 51°30′, 52°30′, and 53°30′ N, respectively. The estimates were calculated for the tsunami wave generation by a seismic source consisting of eight blocks (the second group of calculations, variant 1; see Figure 5b and Table 2).

[42] The four cases of calculation of the tsunami run-up along the Sakhalin coastline are schematically illustrated in Figure 16. An isobath specific to each of the four cases was used for estimating the maximum run-up value by the numerical procedure in use (see points in the figure). Moreover, the wave train that best fitted the given isobath was preliminarily analyzed. We should note that, in all four cases, the first wave in the train is a depressive wave, which implies the possible significant increase in the second or third wave of the train, depending on both parameters of waves arriving at the coast and the geometry of the shelf zone [*Golubtsova and Mazova,* 1989]. The maximum wave heights on the coastline ($R_{\max}$) and on the 10-m isobath ($\eta^{\max}$) at the same latitude are presented in Table 5 (see also Figure 10).

[43] The distinction between $R_{\max}$ and $\eta^{\max}$ is seen to be significant and at some point can reach twofold values.

**Table 5.** Maximum Wave Heights on the Coastline ($R_{\max}$) and the 10-m Isobath ($\eta^{\max}$)

| Latitude | $R_{\max}$ | $\eta^{\max}$ |
|---|---|---|
| 50°00′ | 6.4 | 4.2 |
| 51°30′ | 8.2 | 5.4 |
| 52°30′ | 8.0 | 6.8 |
| 53°30′ | 7.0 | 3.5 |

## Conclusion

[44] The analysis performed in this work has demonstrated that, for the same type of a seismic source, the effect of the motion features of blocks in the source on tsunami manifestations along far-field coastlines of Sakhalin Island and the Kamchatka Peninsula results in both an increase in the run-up value and a significant change in the distribution function of run-up values along a coastline. In contrast, along the near-field coastlines (Kurile Islands), the succession of block movements in the source has a significant effect on the run-up value. Thus, according to computations of various scenarios of the tsunami source formation in the seismic gap zone, the wave heights can reach more than 15 m along coastlines of Kurile-Kamchatka islands, 8 m at several points of the eastern Sakhalin coastline, and 6 m along the Kamchatka coastline.

## Electronic Supplement

[45] The online version of this paper includes Animation 1 showing results of numerical simulation of surface waves generation for the hypothetical seismic source consisting of 8 block-buttons; propagation of tsunami waves up to 10-m isobath. Simultaneous motion of blocks with different velocities and heights was set (see text for more detail).

[46] **Acknowledgments.** This work was supported by the Russian Foundation for Basic Research, project no. 05-05-64685 and by EU Project 502247 (COMSHELFRISKS).

## References

Baranov, B., E. Pristavakina, K. Dozorova, and A. Svarichevsky (1997), The structure of the Okhotsk Sea and the development of its sedimentary basins, *Arctic and Russian Studies II, Report 671,* edited by R. Flecker, p. 58, Cambridge Univ., New York.

Burymskaya, R. N., and A. I. Ivashchenko (1985), Specific features of the wave fields of tsunamigenic earthquakes in the Kurile-Kamchatka zone, in *Theoretical and Experimental Studies of Long Wavelength Processes* (in Russian), p. 9, DVNTs AN SSSR, IMMG, Vladivostok.

Burymskaya, R. N., and V. F. Vyalykh (1985), Motion near the source of the Northern Kuriles earthquake of February 28, 1973, in *Theoretical and Experimental Studies of Long Wavelength Processes* (in Russian), p. 83, DVNTs AN SSSR, IMMG, Vladivostok.

Fedotov, S. A. (1968), On the seismic cycle, quantification of seismic zonation, and long-term seismic prediction, in *Seismic Regionalization of the USSR,* Chapter 8 (in Russian), p. 121, Nauka, Moscow.

Fedotov, S. A., and S. D. Chernyshev (2002), Long-term seismic prediction for the Kurile-Kamchatka arc: Reliability in 1986–2000, development of the method, and prediction for 2001–2005, *Vulkanol. Seismol.* (in Russian), *6,* 3.

Golubtsova, T. S., and R. Kh. Mazova (1989), Coastal run-up on the beach of waves with sign-alternating forms, in *Oscillations and Waves in Continuum Mechanics* (in Russian), p. 30, GPI, Gorki.

Goto, C., Y. Ogawa, N. Shuto, and N. Imamura (1997), *Numerical Method of Tsunami Simulation with the leap-frog scheme, (IUGG/IOC Time Project), IOC Manual, no. 35,* 96 pp., UNESCO, Paris.

Ikonnikova, L. N. (1963), *Atlas of Tsunami* (in Russian), 63 pp., DVNIGMI, Moscow.

Laverov, N. P., S. S. Lappo, L. I. Lobkovsky, and E. A. Kulikov (2006a), Strong Submarine Earthquakes and Catastrophic Tsumamis: Analysis, Modeling, and Prediction, in *Basic Investigations of Oceans and Seas, vol. 1* (in Russian), p. 191, Nauka, Moscow.

Laverov, N. P., S. S. Lappo, and L. I. Lobkovsky (2006b), Central Kurile gap: Structure and seismic potential, *Dokl. Ross. Akad. Nauk* (in Russian), *408,* 818.

Levin, B. V. (1978), A review of studies on the experimental simulation of the tsunami excitation process, in *Methods for Calculating the Tsunami Generation and Propagation* (in Russian), p. 125, Nauka, Moscow.

Lobkovsky, L. I. (1988), *Geodynamics of Spreading and Subduction Zones and Two-Level Plate Tectonics* (in Russian), 253 pp., Nauka, Moscow.

Lobkovsky, L. I., and B. V. Baranov (1984), A keyboard model of strong earthquakes in Island arcs and at active continental margins, *Dokl. Akad. Nauk SSSR* (in Russian), *275*(4), 843.

Lobkovsky, L. I., A. M. Nikishin, and V. E. Khain (2004), *Current Problems of Geotectonics and Geodynamics* (in Russian), 611 pp., Nauchnyi Mir, Moscow.

Lobkovsky, L. I., R. Kh. Mazova, B. V. Baranov, and L. Yu. Kataeva (2006), Generation and propagation of tsunami in the Sea of Okhotsk (possible scenarios), *Dokl. Ross. Akad. Nauk* (in Russian), *410,* 528.

Marchuk, A. G., L. B. Chubarov, and Yu. I. Shokin (1983), *Numerical Simulation of Tsunami Waves* (in Russian), 175 pp., Nauka, Novosibirsk.

Mazova, R. Kh., and J. F. Ramirez (1999), Tsunami waves with an initial negative wave on the Chilean coast, *Natural Hazards, 20,* 83.

Mazova, R. Kh., E. N. Pelinovsky, and S. L. Solovyev (1983), Statistical data on the tsunami wave run-up, *Okeanologiya* (in Russian), *23*(6), 932.

Pelinovsky, E. N. (1982), *Nonlinear Dynamics of Tsunami Waves* (in Russian), 227 pp., IPF AN SSSR, Gorky.

Pelinovsky, E. N., and N. L. Plink (1980), *Preliminary Scheme of the Tsunami zonation along the Kurile-Kamchatka Coastlines from One-Dimensional Calculations with a Model Source,* Preprint no. 5 (in Russian), 21 pp., IPF AN SSSR, Gorky.

Pelinovsky, E. N., and R. Kh. Mazova (1992), Exact analytical solution of nonlinear problems of tsunami wave runup on slopes with different profiles, *Natural Hazards, 6,* 227.

Shchetnikov, N. A. (1990), *Tsunami along Coastlines of the Sakhalin and Kurile Islands from Mareographic Data of 1952–1968* (in Russian), 166 pp., DVNTs AN SSSR, IMMG, Vladivostok.

Solovyev, S. L. (1968), The tsunami problem and its significance for Kamchatka and the Kurile Islands, in *Tsunami Problems* (in Russian), p. 7, Nauka, Moscow.

Solovyev, S. L., Ed. (1978), *Atlas of Maximum Tsunami Run-ups* (in Russian), 61 pp., DVNIGMI, MGI AN SSSR, Vladivostok.

Solovyev, S. L., and I. V. Tulupov (1981), The choice of the scale for the tsunami zonation along a coast, *Okeanologiya* (in Russian), *21*(1), 38.

Solovyev, S. L., A. V. Nekrasov, V. G. Bukhteev, and R. V. Pyaskovsky (1977), Preliminary tsunami zonation along the Kurile- Kamchatka coast from hydrodynamic calculations, in *Theoretical and Experimental Studies of the Tsunami Problem* (in Russian), p. 131, Nauka, Moscow.

Vasilyev, A. A., and N. A. Shchetnikov (1985), Numerical simulation of the Moneron tsunami, in *Theoretical and Experimental Studies of Long Wavelength Processes* (in Russian), p. 122, DVNTs AN SSSR, IMMG, Vladivostok.

Voltsinger, N. E., K. A. Klevanny, and E. N. Pelinovsky (1989), *Long-wavelength dynamics of coastal zone* (in Russian), 272 pp., Hydrometeoizdat, Leningrad.

---

L. I. Lobkovsky, B. V. Baranov, P. P. Shirshov Institute of Oceanology, Russian Academy of Sciences, 36 Nakhimovskiy pr., Moscow, Russia

R. Kh. Mazova, L. Yu. Kataeva, Nizhny Novgorod State Technical University, Nizhny Novgorod, 603600 Russia (raissamazova@mail.nnov.ru)